RNA-dependent sterol aspartylation in fungi

Nathaniel Yakobov[a,1], Frédéric Fischer[a,1,2], Nassira Mahmoudi[a,3], Yusuke Saga[b,3], Christopher D. Grube[c], Hervé Roy[c], Bruno Senger[a], Guillaume Grob[a], Shunsuke Tatematsu[b], Daisuke Yokokawa[b], Isabelle Mouyna[d], Jean-Paul Latgé[d], Harushi Nakajima[b], Tetsuo Kushiro[b], and Hubert D. Becker[a,2]

[a]Université de Strasbourg, CNRS, Génétique Moléculaire, Génomique, Microbiologie, UMR 7156, 67084 Strasbourg Cedex, France; [b]School of Agriculture, Meiji University, Kawasaki 214-8571, Japan; [c]Burnett School of Biomedical Sciences, College of Medicine, University of Central Florida, Orlando, FL 32826; and [d]Unité des Aspergillus, Département de Mycologie, Institut Pasteur, 75724 Paris Cedex 15, France

Edited by Dieter Söll, Yale University, New Haven, CT, and approved May 11, 2020 (received for review February 20, 2020)

Diverting aminoacyl-transfer RNAs (tRNAs) from protein synthesis is a well-known process used by a wide range of bacteria to aminoacylate membrane constituents. By tRNA-dependently adding amino acids to glycerolipids, bacteria change their cell surface properties, which intensifies antimicrobial drug resistance, pathogenicity, and virulence. No equivalent aminoacylated lipids have been uncovered in any eukaryotic species thus far, suggesting that tRNA-dependent lipid remodeling is a process restricted to prokaryotes. We report here the discovery of ergosteryl-3β-*O*-L-aspartate (Erg-Asp), a conjugated sterol that is produced by the tRNA-dependent addition of aspartate to the 3β-OH group of ergosterol, the major sterol found in fungal membranes. In fact, Erg-Asp exists in the majority of "higher" fungi, including species of biotechnological interest, and, more importantly, in human pathogens like *Aspergillus fumigatus*. We show that a bifunctional enzyme, ergosteryl-3β-*O*-L-aspartate synthase (ErdS), is responsible for Erg-Asp synthesis. ErdS corresponds to a unique fusion of an aspartyl-tRNA synthetase—that produces aspartyl-tRNA^{Asp} (Asp-tRNA^{Asp})—and of a *Domain of Unknown Function 2156*, which actually transfers aspartate from Asp-tRNA^{Asp} onto ergosterol. We also uncovered that removal of the Asp modifier from Erg-Asp is catalyzed by a second enzyme, ErdH, that is a genuine Erg-Asp hydrolase participating in the turnover of the conjugated sterol in vivo. Phylogenomics highlights that the entire Erg-Asp synthesis/degradation pathway is conserved across "higher" fungi. Given the central roles of sterols and conjugated sterols in fungi, we propose that this tRNA-dependent ergosterol modification and homeostasis system might have broader implications in membrane remodeling, trafficking, antimicrobial resistance, or pathogenicity.

aminoacyl-tRNA | ergosterol | fungi | DUF2156 | lipid aminoacylation

Remodeling of membranes and lipid modifications are processes used by living cells to interact with and adapt to their environment. They are notably critical for host/pathogens interactions, antimicrobial resistance, and virulence in both bacteria (1, 2) and fungi (3). MprFs are bacterial virulence factors that transfer amino acids (aa) onto membrane glycerolipids in a so-called aminoacylation reaction (4). This process requires aminoacyl-transfer RNAs (aa-tRNA) that are first synthesized by aminoacyl-tRNA synthetases (aaRS) (5), prior transfer of the aa moiety onto a lipid acceptor substrate, that is, phosphatidylglycerol, cardiolipin, or diacylglycerol (4). The aminoacyl-tRNA transferase (AAT) module, that catalyzes the transfer, belongs to the DUF2156 family and recognizes both the aa-tRNA and the lipid substrates (6). Glycerolipid aminoacylation modifies the overall charge, fluidity, and permeability of bacterial membranes, which enhances antimicrobial resistance, explaining why these enzymes have been termed multiple peptides resistance factors (MprF) (4). Glycerolipid aminoacylations also affect host/pathogen interactions and have been shown to potentiate immune escape and to increase virulence of pathogens (7). In *Pseudomonas aeruginosa* (8), *Enterococcus faecium* (9), and *Agrobacterium tumefaciens* (10), extracytoplasmic esterases of the VirJ or α/β-hydrolase family participate in the homeostasis of aminoacylated lipids and hydrolyze the modifying aa from lipids.

So far, only glycerolipids have been shown to be aminoacylated and only by MprFs in prokaryotes. In the present study, we show that eukaryotes aminoacylate sterols in a tRNA-dependent modification pathway that mimics those described in bacteria. In higher fungi, we functionally characterized a novel enzyme, the ergosteryl-3β-*O*-L-aspartate synthase (ErdS), composed of a DUF2156/AAT domain fused to an aspartyl-tRNA synthetase (AspRS) paralog. We show that ErdS synthesizes ergosteryl-3β-*O*-L-aspartate (Erg-Asp), a previously undetected conjugated sterol. Moreover, most of higher fungi (Dikarya), including opportunistic human pathogens such as *Aspergillus fumigatus* (*Afm*), encode this ErdS and produce Erg-Asp, suggesting that the system is widespread in "higher" fungi. We also evidenced that these species express a dedicated Erg-Asp hydrolase (ErdH) that deacylates Erg-Asp and whose gene is almost always located in a two-gene cluster next to the *erdS* gene. In conclusion, our data unravel an evolutionary conserved sterol−aa conjugation pathway. We discuss the potential implications of this pathway in the context of lipid homeostasis and antimicrobial resistance.

Significance

Bacteria are known to add amino acids (aa) to membrane lipids to resist antimicrobials and escape immune responses. This surface lipid aminoacylation process requires diverting aminoacyl-tRNAs from protein synthesis. While widespread in bacteria, no analogous lipid remodeling system had thus far been evidenced in eukaryotes. We uncovered that most fungi tRNA-dependently add aspartate onto ergosterol (ergosteryl-3β-*O*-L-aspartate [Erg-Asp]), the major sterol found in fungal membranes. Asp addition is catalyzed by an ergosteryl-3β-*O*-L-aspartate synthase (ErdS) and its removal by a dedicated hydrolase (ErdH). This pathway is conserved across "higher" fungi, including pathogens. Given the central roles of sterols and derivatives in fungi, we propose that the Erg-Asp homeostasis system might impact membrane remodeling, trafficking, antimicrobial resistance, or pathogenicity.

Author contributions: F.F., T.K., and H.D.B. designed research; N.Y., F.F., N.M., Y.S., C.D.G., H.R., S.T., D.Y., and H.N. performed research; N.Y., F.F., N.M., Y.S., C.D.G., H.R., G.G., S.T., D.Y., I.M., J.-P.L., and H.N. contributed new reagents/analytic tools; N.Y., F.F., N.M., Y.S., C.D.G., H.R., B.S., G.G., S.T., D.Y., I.M., J.-P.L., H.N., T.K., and H.D.B. analyzed data; N.Y., F.F., N.M., H.R., B.S., G.G., T.K., and H.D.B. wrote the paper; and H.D.B. coordinated research.

The authors declare no competing interest.

This article is a PNAS Direct Submission.

This open access article is distributed under Creative Commons Attribution-NonCommercial-NoDerivatives License 4.0 (CC BY-NC-ND).

[1]N.Y. and F.F. contributed equally to this work.

[2]To whom correspondence may be addressed. Email: frfischer@unistra.fr or h.becker@unistra.fr.

[3]N.M. and Y.S. contributed equally to this work.

This article contains supporting information online at https://www.pnas.org/lookup/suppl/doi:10.1073/pnas.2003266117/-/DCSupplemental.

First published June 15, 2020.

Downloaded by guest on September 16, 2020

Results

DUF2156 Proteins Are Present in Fungi. Although DUF2156 domains were thought to be absent or rare outside prokaryotes (11), we identified, in most higher fungi, DUF2156-containing proteins fused to the C terminus of an aaRS-like domain (Fig. 1*A* and *SI Appendix*, Fig. S1*A*), that we named ErdS for reasons that will be presented below. This protein architecture, previously detected in two fungi (12), is actually widespread across fungi, including the well-characterized *Afm*, *Aspergillus oryzae* (*Aor*), or *Neurospora crassa* (*Ncr*) (Fig. 1*A*). Firstly, sequence analyses and structure predictions of the detected DUF2156 domains suggested that they all adopt the characteristic double Gcn5-like *N*-acetyltransferase (GNAT) fold observed in bacterial MprFs (6). In fungal DUF2156 domains, the GNAT I (recognition of the acceptor substrate) and II (transferase activity) subdomains of the double GNAT fold are separated, like in bacteria, by a positively charged $\alpha^{(+)}$ helix involved (Fig. 1 *A* and *B*) in the binding of aa-tRNAs (6), suggesting that 1) they could indeed be aa-tRNA–utilizing modules and 2) they might transfer the aa moiety of aa-tRNAs onto lipids. Second, the aaRS domains contain bona fide AspRS signature sequences including the known residues (13) involved in $tRNA^{Asp}$, Asp, and adenosine 5′-triphosphate (ATP) binding ubiquitously found in functional AspRSs (*SI Appendix*, Fig. S1*B*). These considerations prompted us to propose the following working hypothesis: The AspRS domain of ErdS would generate Asp-$tRNA^{Asp}$ from ATP, L-Asp, and $tRNA^{Asp}$, which would then be transferred to the DUF2156 module, thought to carry the AAT activity, to transfer the Asp residue onto a yet-to-be identified lipid (Fig. 1*C*).

ErdS Is Essential for the Synthesis of a Lipid in Filamentous Fungi. In order to test our hypothesis on the function of ErdSs, we deleted the corresponding *erdS* genes in two fungi (Fig. 2*A* and *SI Appendix*, Fig. S2), namely, the human opportunistic pathogen *Afm* and the species of biotechnological and industrial interest *Aor*. Both Δ*erdS* mutants grew normally on solid media (*SI Appendix*, Fig. S3), demonstrating that the genes are not essential under standard growth conditions. To visualize whether ErdSs are involved in lipid aminoacylation, we analyzed total lipids from mycelia of the wild-type (WT) and *ΔerdS* strains by thin-layer chromatography (TLC), and results revealed, in both fungi, the presence of an additional ErdS-dependent lipid (hereafter, lipid X or LX) with a distinctive brownish staining that migrates between phosphatidylethanolamine (PE) and phosphatidylcholine (PC) (Fig. 2 *B* and *C*).

To verify the ErdS dependency of LX synthesis, we constructed an *Afm* Δ*erdS*::P_{xyl}-*erdS* strain, in which we reintroduced the WT *erdS* gene under the control of a xylose (Xyl)-inducible promoter (P_{xyl}-*erdS*) at the *ΔerdS* locus (Fig. 2*A* and *SI Appendix*, Fig. S2). Under noninduced conditions (in the presence of glucose), LX was barely undetectable in the Δ*erdS*::P_{xyl}-*erdS* strain compared to the WT, while, under induction conditions (in the presence of Xyl), strong accumulation of LX occurred (Fig. 2*B*). In *Aor*, complementation of the Δ*erdS* mutation with the WT *erdS* copy (Fig. 2*A*) at an ectopic locus under the control of its own promoter again restored LX synthesis (Fig. 2*C*), which proved that LX synthesis is dependent on ErdS expression. Interestingly, only the full-length ErdS could sustain efficient LX synthesis in *Aor*, while an ErdS mutant in which the AspRS domain was deleted (Fig. 2*C*, Δ*erdS*+*erdS-ΔaspRS*) could not, at least not at detectable levels.

Fungal ErdS Catalyzes tRNA-Dependent Aspartylation of a Lipid. To dissect the mechanism of LX synthesis, we transferred the synthesis of LX, hypothesized to rely on the sole ErdS enzyme, to the budding yeast *Saccharomyces cerevisiae* (*Sce*), in which we overexpressed *Afm* ErdS. Switching to a heterologous yeast system was dictated for three main reasons: 1) Genetic engineering is far more time consuming in *Afm* than in *Sce*; 2) no DUF2156-containing proteins were detected in *Sce* (*SI Appendix*, Fig. S1*A*); and 3) the lipid synthesis pathways are conserved across ascomycetes (amigo.geneontology.org/amigo/term/GO:0006629), and thus the lipid contents of these species belonging to the same phylum are likely to be very similar (14). To start with and test whether the AspRS moiety was functional, *Afm* ErdS or ErdS-ΔDUF, that is an ErdS form that comprises only the AspRS domain, was expressed in the *Sce* Δ*dps1* strain (15) (*DPS1* encodes the essential AspRS), and complementation of the Δ*dps1* mutation lethality was tested by plasmid shuffling (Fig. 3*A* and *SI Appendix*, Fig. S4*A*). Results show that both ErdS and ErdS-ΔDUF functionally replaced *Sce* AspRS in vivo. This was not observed with a catalytic null mutant ($ErdS_{AAPA}$) of the AspRS domain (Fig. 3*A* and *SI Appendix*, Fig. S4*A*), in which the QSPQ signature motif (16) was mutated to AAPA. In addition, in vitro aminoacylation assays with purified recombinant *Afm* ErdS and *Sce* $tRNA^{Asp}$ confirmed ErdS's capacity to generate Asp-$tRNA^{Asp}$ (*SI Appendix*, Fig. S4*B*). Interestingly, full-length ErdS displays a lower complementation efficiency of the *Sce Δdps1* strain compared to ErdS-ΔDUF (*SI Appendix*, Fig. S4*A*). We interpreted that, in the full-length ErdS, the DUF2156 domain likely transfers

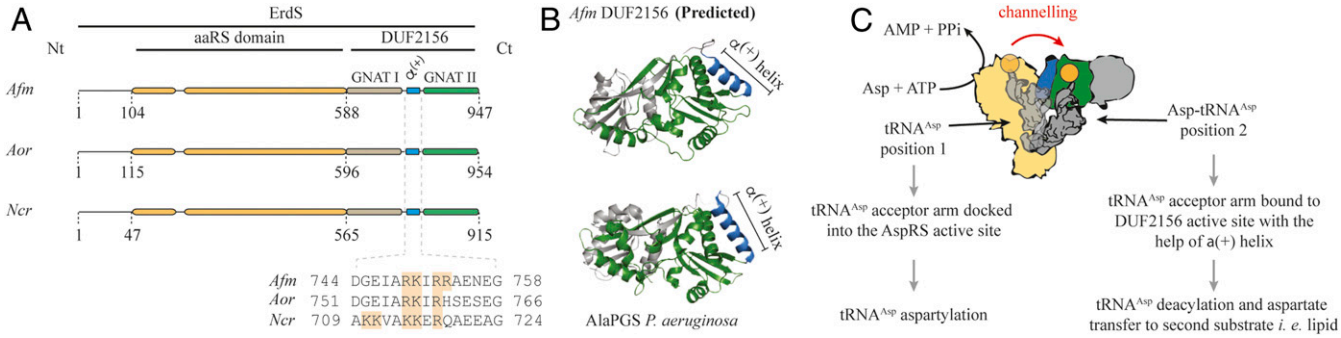

Fig. 1. Filamentous fungi AspRS-DUF2156, proteins termed ErdSs, are potential lipid aminoacylation factors. (*A*) *In silico* analyses predicted *Afm*, *Aor*, or *Ncr erdS* genes to encode proteins composed of an AspRS domain N-terminally fused to a DUF2156 domain. Protein domains were delimited by confronting data obtained from Protein Families database (PFAM) and from multiple alignments as described in *SI Appendix, Supplementary Materials and Methods*. Critical positively charged residues in the alpha helix ($\alpha^{(+)}$) separating both GNAT folds are indicated (orange). (*B*) Comparison of the DUF2156 structure of AlaPGS (alanyl-phosphatidylglycerol synthase, MprF) from *P. aeruginosa* to the Phyre2 prediction of *Afm* DUF2156. GNAT I and II subdomains are highlighted in gray and green, respectively, with the positively charged $\alpha^{(+)}$ helix in blue. (*C*) Schematic representation of the hypothetical ErdS reaction mechanism during which $tRNA^{Asp}$ shift from the AspRS catalytic site (position 1: $tRNA^{Asp}$ aspartylation) to the DUF2156 active site (position 2: Asp transfer from Asp-$tRNA^{Asp}$ onto a lipid substrate). The $\alpha^{(+)}$ helix is indicated in blue, and the active site is indicated in green. Aspartate is represented in orange.

BIOCHEMISTRY

Downloaded by guest on September 16, 2020

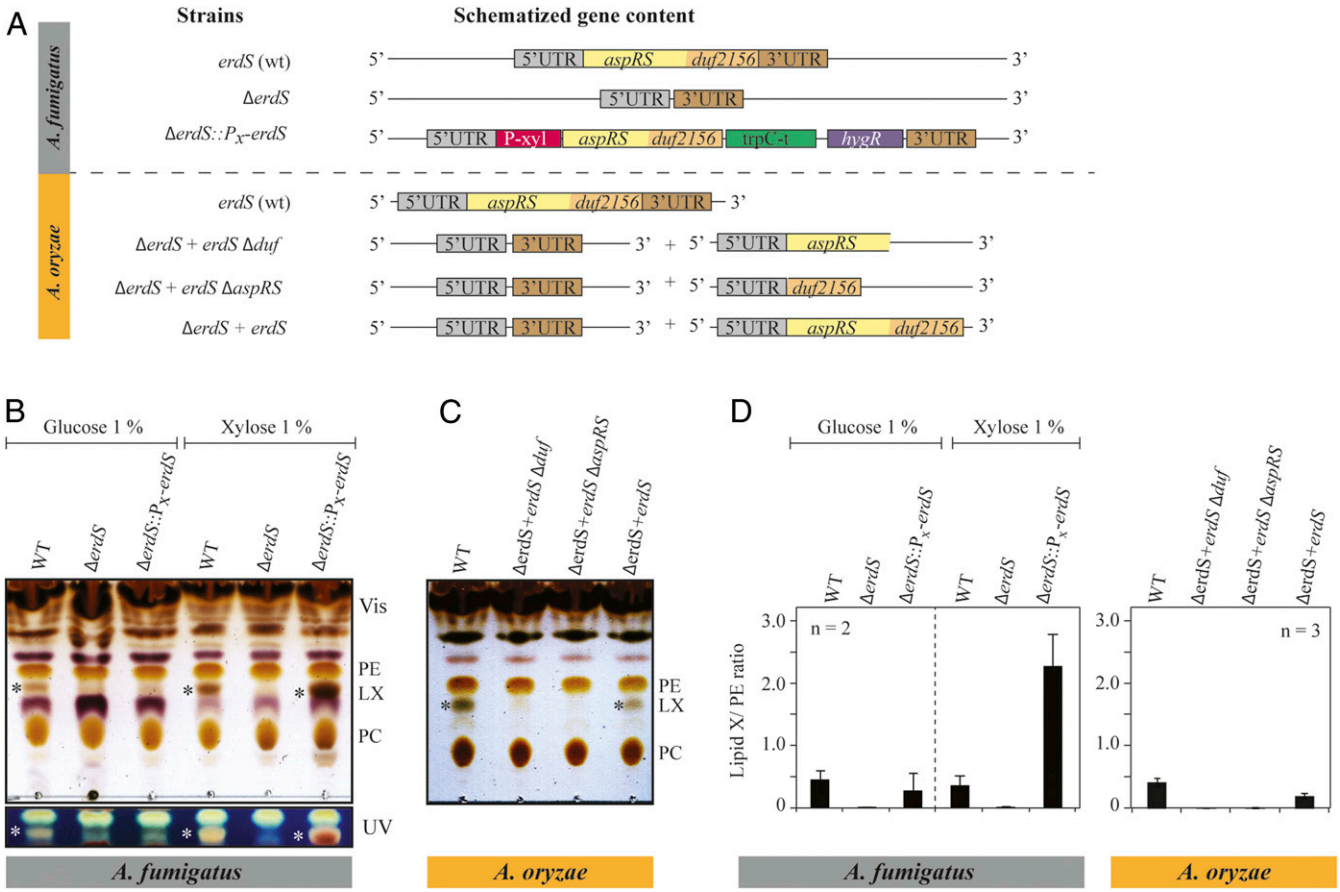

Fig. 2. Identification of an *Aspergillus* lipid species, whose synthesis requires ErdS. (*A*) Deletions of *erdS* from *Afm* and from *Aor* were performed by homologous recombination (see *SI Appendix* for details). The genotypes of the strains are indicated. For *Afm*, the *ΔerdS* strain shown corresponds to the strain after excision of the deletion cassette, whereas, for the complemented *ΔerdS*::P_X-*erdS* strain, the selection marker is still present. For *Aor*, the ORF of *erdS* was replaced by a *pyrG*-containing module and subsequently excised by selection on 5-FOA medium. Complementation was operated by ectopic expression of *erdS-ΔDUF*, *erdS-ΔAspRS*, or *erdS*. (*B* and *C*) Total lipids extracted from the different strains described in *A* were analyzed by TLC and stained with a sulfuric acid/$MnCl_2$ solution. TLC plates were observed either under white light or under UV light. Cultures were done in glucose or xylose containing media; * indicates the LX. (*D*) Quantification of the TLCs shown in *B* and *C*. LX signal (number of pixels) was normalized to that of PE (phosphatidylethanolamine) (LX/PE ratio). All TLCs are representative of at least two independent experiments ($n = 2$).

Asp from Asp-tRNA^{Asp} onto an accepting lipid, thereby decreasing the amount of Asp-tRNA^{Asp} available for protein synthesis and impacting growth.

To determine whether the DUF2156 module of ErdS transfers Asp from Asp-tRNA^{Asp} onto lipids in vivo, as suggested from the results obtained in *Aspergillus* spp. (Fig. 2 *B* and *C*), we analyzed the total lipid composition of a WT *Sce* strain bearing plasmids that express *Afm* or *Aor* full-length or truncated ErdSs (Fig. 3*A*). Expression of proteins was confirmed by Western blot with anti-ErdS antibodies that recognize both *Afm* and *Aor* ErdS (Fig. 3*B*), and analyses of total lipids by TLC revealed the presence of an additional brownish lipid, absent in WT *Sce* strains, when *Afm* and *Aor* ErdS were expressed. This lipid presents the same migration profile as the LX detected in *Afm* and *Aor* (*SI Appendix*, Fig. S4*C*), strongly suggesting that heterologous expression of *Afm* or *Aor* ErdS in *Sce* allows complete and correct synthesis of LX. Positive staining of LX with ninhydrin (detection of primary amine) and bromocresol green (detection of carboxyl) further suggested that it contained an aa moiety, likely L-Asp ester- or amide-linked through its α-carboxyl the lipid moiety, with free α-NH_3^+ and β-COO^- groups (*SI Appendix*, Fig. S4*D*).

To investigate whether ErdS transfers Asp from Asp-tRNA^{Asp} onto a lipid in a DUF2156-dependent manner, we analyzed the total lipids produced by ErdS-ΔDUF, ErdS-ΔAspRS, and $ErdS_{AAPA}$ expressed in *Sce* (Fig. 3*B*). Expression of the different constructs was confirmed by anti-ErdS Western blot (Fig. 3*B*). The ErdS-ΔDUF could not be detected, because our antibodies were raised against the DUF2156 domain; however, complementation of the lethal *Δdps1* mutation in *Sce* by ErdS-ΔDUF confirmed that the AspRS moiety was expressed and functional (*SI Appendix*, Fig. S4*A*). LX spots were quantified and normalized to those of PE (LX/PE ratio, presented in Fig. 3*B*). Of note is that, in the absence of LX, PG becomes visible at the same position in *Sce*, a reason for which the PG/PE ratio was used as a "background" signal (Fig. 3*B*, gray background). LX was not observed in *Sce* upon removal of the DUF2156 domain from ErdS (LX/PE ratio similar to the PG/PX ratio of the WT strain), and expression of the DUF2156 domain *in trans* in the *Sce*+ErdS-ΔDUF strain restored LX synthesis (Fig. 3*B*, *Sce*+ΔA+ΔD), although at lower levels, with an LX/PE ratio close to that of the PG/PE ratio of the WT strain. Only the specific brown staining of LX confirmed its low-level production. These data demonstrate that synthesis of LX is DUF2156 dependent. The reduced level of LX in the *Sce*+ErdS-ΔAspRS strain, despite proper expression of the enzyme, shows that the lipid synthesis activity of the standalone DUF2156 domain is weaker than when fused to its AspRS moiety (low LX/PE ratio), which recalls results obtained in *Aor* (Fig. 2*C*). Similarly, in the

Downloaded by guest on September 16, 2020

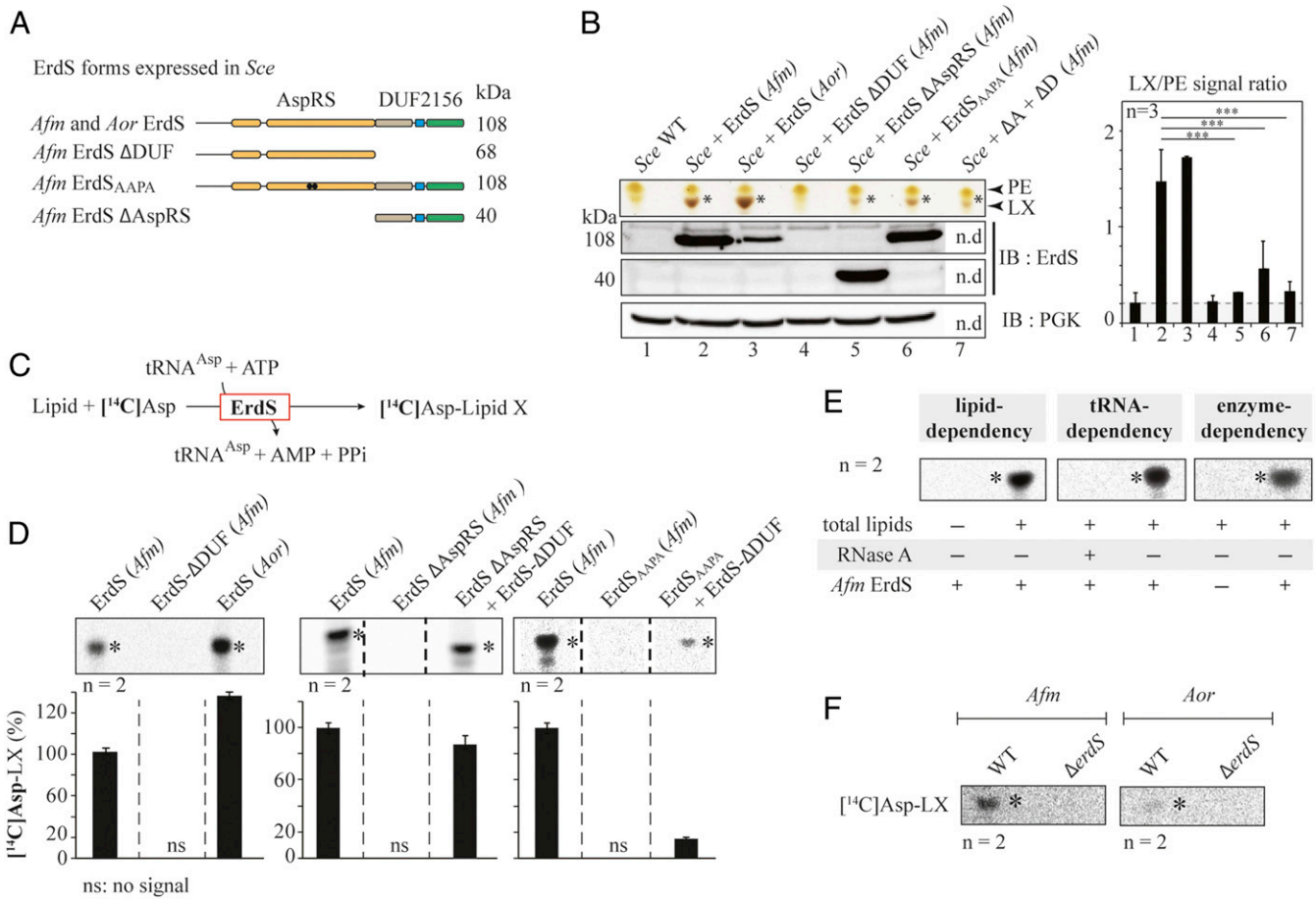

Fig. 3. Dissecting ErdS lipid modification mechanism. (*A*) Schematized modular organization of full-length ErdS (108 kDa, *Afm* and *Aor*) and of its variants (*Afm*) that were expressed in the *Sce* heterologous model. ErdS-ΔDUF: AspRS standalone domain; ErdS-ΔAspRS: DUF2156 standalone domain (40 kDa); $ErdS_{AAPA}$: catalytic null of the AspRS moiety (108 kDa). (*B*) TLC-based analysis of total lipids from *Sce* expressing ErdS variants described in *A* and *Sce* + (ΔD + ΔA) corresponds to the double expression of ErdS-ΔDUF + ErdS-ΔAspRS in *Sce*. The TLC plate stained with sulfuric acid/$MnCl_2$ was cropped to the area of interest. LX signal (number of pixels) was normalized to that of PE in each case, and the LX/PE ratio is represented in a graph (*Right*). In the absence of LX, PG (phosphatidylglycerol) becomes visible; thus the PG/LX ratio obtained was considered "background signal" (gray background). However, the brown staining of LX (yellow for PG) made it possible to visually assess the presence of LX even for low LX/PE values. The Student's *t* test was used to assess the significance of the means of the data; ***$P < 0.005$. ErdS variants expression was analyzed by Western blot with an anti-*Afm* DUF2156 polyclonal antibodies (IB:ErdS), and loading control was performed with anti-PGK antibodies (IB:PGK). (*C*) Schematized reaction of the LA assay, described in *Materials and Methods*. (*D*) LX synthesis by the purified recombinant full-length and mutant ErdSs was measured using the LA assay. When mixed, proteins were in equimolar ratios. The [^{14}C]-Asp lipid levels (percent) are provided below each TLC. (*E*) Verification of tRNA, lipid, and ErdS dependency of LX synthesis using LA assay; +: presence; –: absence. (*F*) Measurements of lipid X synthesis (ErdS activity) by WT and Δ*erdS Aspergillus* spp. crude extracts using LA assay; *: LX. The [^{14}C]Asp lipids were revealed using phosphorimaging (*D*–*F*). TLCs and immunoblots are representative of two to three independent experiments, and the number of replicates (*n*) is indicated.

Sce strain that expresses ErdS with a catalytically null AspRS moiety (*Sce*+$ErdS_{AAPA}$), LX levels mirrored those of the *Sce*+ErdS-ΔAspRS and *Sce*+ΔA+ΔD strains (Fig. 3*B*). These experiments show, in addition, that the DUF2156 domain of ErdS can efficiently utilize *Sce* Asp-$tRNA^{Asp}$, regardless of whether it was generated by the *Afm* AspRS moiety of ErdS or by the endogenous *Sce* AspRS.

To better characterize the ErdS catalytic mechanism, we developed an in vitro lipid aminoacylation assay (LA assay), using purified *Afm* or *Aor* recombinant ErdS incubated with purified *Sce* $tRNA^{Asp}$, ATP, and [^{14}C]-Asp in the presence of *Sce* total lipids (Fig. 3*C*). Reaction products from the LA assay were analyzed by TLC (Fig. 3 *D* and *E*). Results confirmed that *Afm* or *Aor* recombinant ErdSs catalyzed the formation of a [^{14}C]-labeled lipid (Fig. 3*D*). Adding RNase or removing lipids from the LA assay abolished synthesis of [^{14}C]-lipid, thereby proving the tRNA and lipid dependency of LX synthesis by *Afm* ErdS (Fig. 3*E*). When the recombinant *Afm* ErdS-ΔDUF protein was used, synthesis of the [^{14}C]-lipid was abolished, proving that the reaction is, indeed, DUF2156 dependent (Fig. 3*D*). Likewise, when ErdS-ΔAspRS or $ErdS_{AAPA}$ were used in the LA assay, synthesis of the [^{14}C]-lipid was abolished (Fig. 3*D*), but fully restored upon addition of the AspRS domain of ErdS *in trans*. These data confirm results obtained in *Sce* but also that the DUF2156 is capable of capturing Asp-$tRNA^{Asp}$ formed by an AspRS expressed *in trans* (Fig. 3*D*).

Finally, crude extracts from WT *Afm* or *Aor* mycelia also catalyzed a [^{14}C]-Asp-$tRNA^{Asp}$–dependent [^{14}C]-lipid synthesis in vitro, whereas crude extracts from Δ*erdS* mutant strains did not (Fig. 3*F*). However, for reasons that will be discussed below, the ErdS activity was hardly detectable in crude extracts, especially for *Aor*, when compared to recombinant ErdS.

Altogether, these results show that ErdS produces Asp-$tRNA^{Asp}$ from ATP, L-Asp, and $tRNA^{Asp}$ in its AspRS domain,

BIOCHEMISTRY

Downloaded by guest on September 16, 2020

and that the Asp-tRNA^{Asp} product likely shifts from the AspRS active site to the DUF2156 module, that transfers the Asp acylating tRNA^{Asp} onto a lipid, which mirrors the activity of bacterial DUF2156 proteins (4).

Liquid chromatography-MS/MS Reveals that ErdS Aspartylates Ergosterol. To identify the substrate lipid of ErdS, we fractionated total lipids from an ErdS overexpressing *Sce* strain by column chromatography and isolated LX at ~80% purity (*SI Appendix*, Fig. S5*A*). Fractions were submitted to mass spectrometry (MS) analyses and compared to equivalent fractions obtained from total lipids of a WT yeast strain. Strikingly, MS electrospray ionization quadrupole time-of-flight (MS-ESI-QTOF) spectra revealed two peaks, absent in WT fractions, with *m*/*z* of 379.3380 and 534.3565 that were submitted to a second round of MS/MS collision-induced dissociation QTOF (MS/MS-CID-QTOF) (Fig. 4*A*). Contrary to bacterial MprF-aminoacylated lipids, results were not compatible with LX being a glycerolipid derivative. Fragmentation pattern of the first peak was rather consistent with a dehydrated ergosterol (Erg) (*m*/*z* 379.3355), which was supported by the presence of characteristic additional Erg fragmentation products (Fig. 4*A*) (17). The second peak gave similar fragmentation products together with that of Asp (*m*/*z* of 156.0265, $[C_4H_7NO_4Na]^+$) and of an aspartylated form of Erg (534.3547, $[M{\sim}aspartyl{+}Na]^+$). Results were consistent with an Erg moiety esterified with Asp on the β-OH group in position 3 of the A ring, making this species an Erg-Asp (Fig. 4*B*). Finally, liquid chromatography (LC)-ESI-MS/MS analyses of total lipids extracted directly from *Afm* confirmed that Erg-Asp was indeed present (*SI Appendix*, Fig. S5*B*). In parallel, we chemically synthesized Erg-Asp that we compared, on TLC, to Erg-Asp present in total lipids of *Afm*, *Aor*, or *Sce* expressing *Afm* ErdS and confirmed that, as expected, it shared the exact same migration properties (*SI Appendix*, Fig. S6).

To confirm that Erg is the substrate of ErdS, we performed LA assays using either [^{3}H]-Erg and cold Asp or cold Erg and [^{14}C]-Asp. Analyses of reaction products by TLC revealed that ErdS indeed produced [^{3}H]-Erg-Asp (Fig. 4*C*) or [^{14}C]-Erg-Asp (Fig. 4*D*) in a tRNA-dependent manner, and that it requires L-Asp, ATP, and tRNA^{Asp} for activity. Interestingly, in the presence of cholesterol (Cho), the animal equivalent of Erg and [^{14}C]-Asp, ErdS also produced cholesteryl-aspartate (Cho-Asp) (Fig. 4*D*), indicating that it likely has a relaxed specificity toward

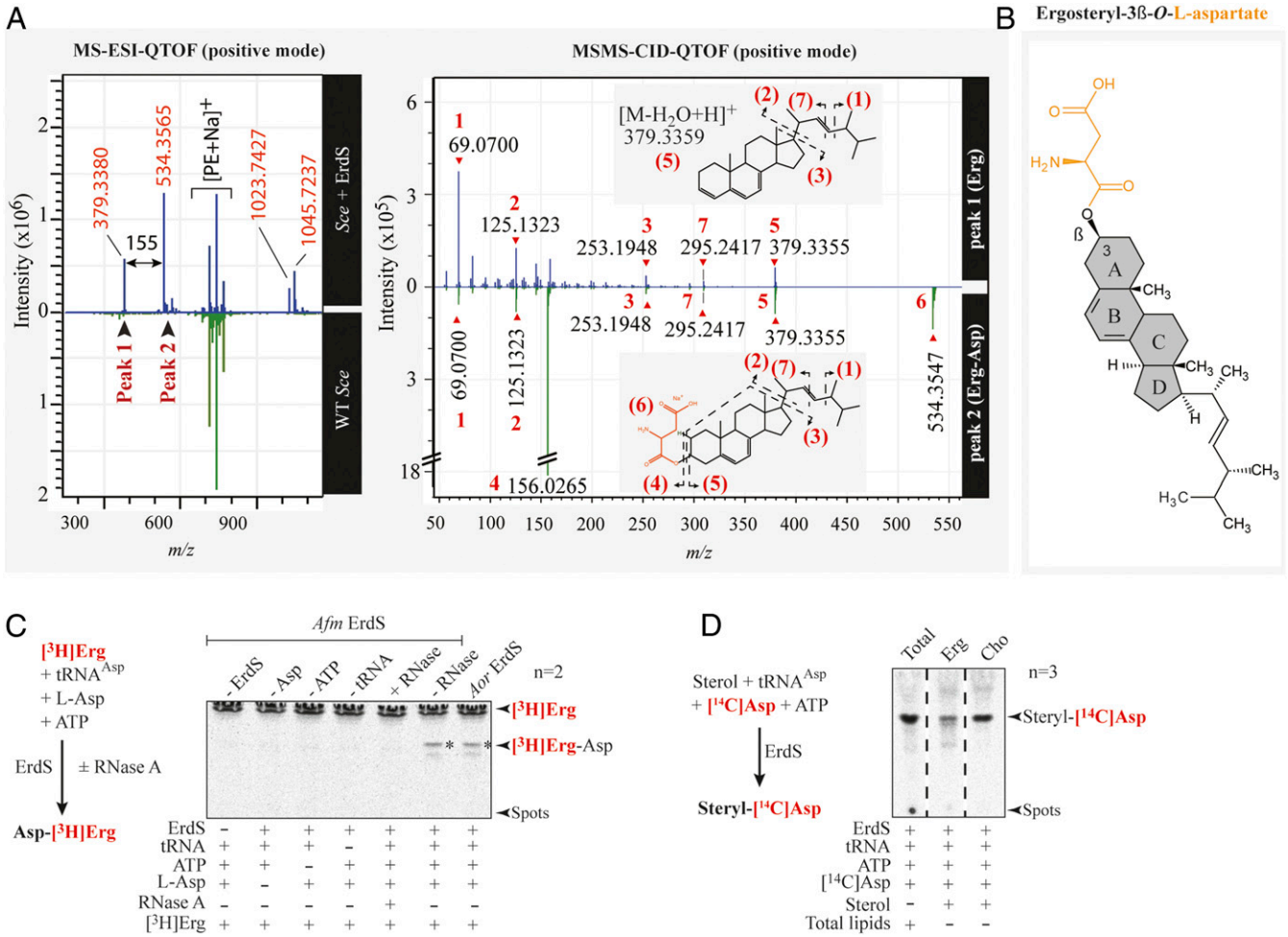

Fig. 4. Identification of the ergosteryl-3β-*O*-L-aspartate produced by ErdS in vivo and in vitro. (*A*) MS-ESI-QTOF spectrum (positive mode) of a lipid fraction containing LX extracted and purified from an *Sce* WT strain expressing *Afm* ErdS (upper spectrum, blue) or not (bottom spectrum, green). Peaks 1 and 2 have been analyzed by MS/MS collision-induced dissociation (CID) QTOF analysis in the positive mode. (*B*) Chemical structure of ergosteryl-3β-*O*-L-aspartate (Erg-Ap) corresponding to LX deduced from MS spectra shown in *A*. (*C*) The [^{3}H]Erg-Asp synthesis was measured by LA assay in the presence of purified *Afm* ErdS, pure *Sce* tRNA^{Asp}, radiolabeled [^{3}H]Erg, and cold Asp in the presence (+) or absence (–) of the enzyme or of the indicated substrates. Tests included addition (+) or not (–) of RNase A. [^{3}H]Erg-Asp is indicated with an asterisk. (*D*) Erg-[^{14}C]Asp synthesis measured by LA assay using purified *Afm* ErdS, pure *Sce* tRNA^{Asp}, radiolabeled [^{14}C]Asp, and indicated sterols. LA assay using total lipids from WT *Sce* was used as a migration control. The adapted LA assay reactions are displayed (simplified) next to the corresponding TLCs. Radiolabeled compounds are highlighted in red, and the number of independent experiments (*n*) is indicated.

Downloaded by guest on September 16, 2020

its sterol substrate. Overall, our results demonstrate that ErdSs represent a novel type of bifunctional AspRS/ergosteryl-aspartate synthases that we named ergosteryl-3β-*O*-L-aspartate synthases or ErdS, with "Er" standing for "ergosteryl," "d" for Asp, and "S" for synthase.

Fungi Having ErdS also Encode a Dedicated Erg-Asp Hydrolase Involved in Erg-Asp Turnover. Bacteria that possess MprFs are also equipped with dedicated hydrolases that remove aa modifiers from lipids, and whose gene usually lays next to *mprF* genes (8, 9). In *Afm*, *Aor*, and *Ncr*, we observed that the *erdS* gene (*AFUA_1g02570* in *Afm* Af293, *AO090005000838* in *Aor* RIB40, and *NCU007082* in *Ncr* OR74A) is found close to a gene encoding a protein belonging to the α/β-hydrolase family (PFAM: PF07859) (*AFUA_1g02580*, *AO090005000837*, and *NCU007081*, respectively) (Fig. 5*A*). These α/β-hydrolases all contain three conserved residues, Ser153, Asp277, and His307 (numbering of *Afm*), that are typical of the catalytic triad of esterases/lipases, a finding supported by structure predictions (Fig. 5*A*).

To determine whether these esterases were involved in the Erg-Asp metabolic pathway, we used *Ncr* because, in this fungus, despite the presence of an *erdS* gene (Fig. 5*A* and *SI Appendix*, Fig. S1*A*), we could not observe Erg-Asp in total lipids, although an ErdS activity could be detected using the LA assay in crude protein extracts (*SI Appendix*, Fig. S7). The WT, Δ*erdS*, and Δ*esterase* deletion mutants of *Ncr* were obtained from the Fungal Genetic Stock Center (FGSC) (18, 19). We compared total lipids profiles of *Ncr* WT, Δ*erdS*, and Δ*esterase* mutants by TLC (Fig. 5*B*). As stated, Erg-Asp was undetectable in the WT or Δ*erdS* strains of *Ncr* but accumulated at high levels in the Δ*esterase* strain (Fig. 5*B*), suggesting that the enzyme was most likely responsible for the absence of detectable Erg-Asp in WT *Ncr*. This esterase, seemingly involved in Erg-Asp degradation, was therefore named ErdH, for Erg-Asp hydrolase, and the Δ*esterase* strain was renamed Δ*erdH* (Fig. 5 *A* and *B*). Additionally, we monitored the Erg-[^{14}C]-Asp synthesis activity by LA assay in protein extracts from WT *Ncr*, Δ*erdS*, and Δ*erdH* strains. Our data show that, while almost undetectable under the conditions tested in the WT and Δ*erdS* strains, Erg-[^{14}C]-Asp levels were much higher (>23-fold) in the Δ*erdH* strain (Fig. 5*C*). This is again in agreement with ErdH being involved in Erg-Asp deacylation, which most likely masked the Erg-Asp synthesis activity of ErdS in the WT *Ncr* strain. Similarly, Erg-Asp synthesis was hardly monitored in vitro using total protein extracts of *Afm* and *Aor* (Fig. 3*F*), suggesting either low expression levels of ErdS or that ErdH hydrolyzed the Erg-Asp product.

In order to confirm that ErdH was indeed an Erg-Asp hydrolase, we used an in vitro Erg-Asp deacylation assay. Erg-[^{14}C]-Asp incubated for 30 min with purified recombinant *Afm* ErdH was almost entirely hydrolyzed (88 ± 2%), while, in the same reaction performed without ErdH, Erg-[^{14}C]-Asp levels remained stable (Fig. 5*D*). In addition, purified ErdH mutants of the catalytic triad (S153A, D277A, or H307A) did not hydrolyze Erg-[^{14}C]-Asp in vitro (Fig. 5*D*). All these results demonstrate the presence of two enzymes in fungi that regulate the synthesis and degradation of Erg-Asp, namely ErdS and ErdH.

An Evolutionary Conserved Synteny between *erdS* and *erdH*. ErdS and ErdH are present in *Afm*, *Aor*, and *Ncr*, with their respective genes found at the same locus and encoded as divergent expression units. In order to analyze whether ErdS and ErdH are more generally found in fungi and/or other eukaryotes, we performed bioinformatics searches (*SI Appendix*, *Supplemental Materials and Methods*). We first searched ErdS sequences among eukaryotes using the basic local alignment search tool (BLAST) with the *Afm* ErdS sequence as a probe and found 7,584 protein sequences (only those with lengths 200 to 2,000 residues), that corresponded to ErdS, standalone DUF2156 domains, canonical AspRSs, and homologous aaRSs such as asparaginyl- and lysyl-tRNA synthetases. Among them, 1,006 (13.3%) were bona fide DUF2156-containing

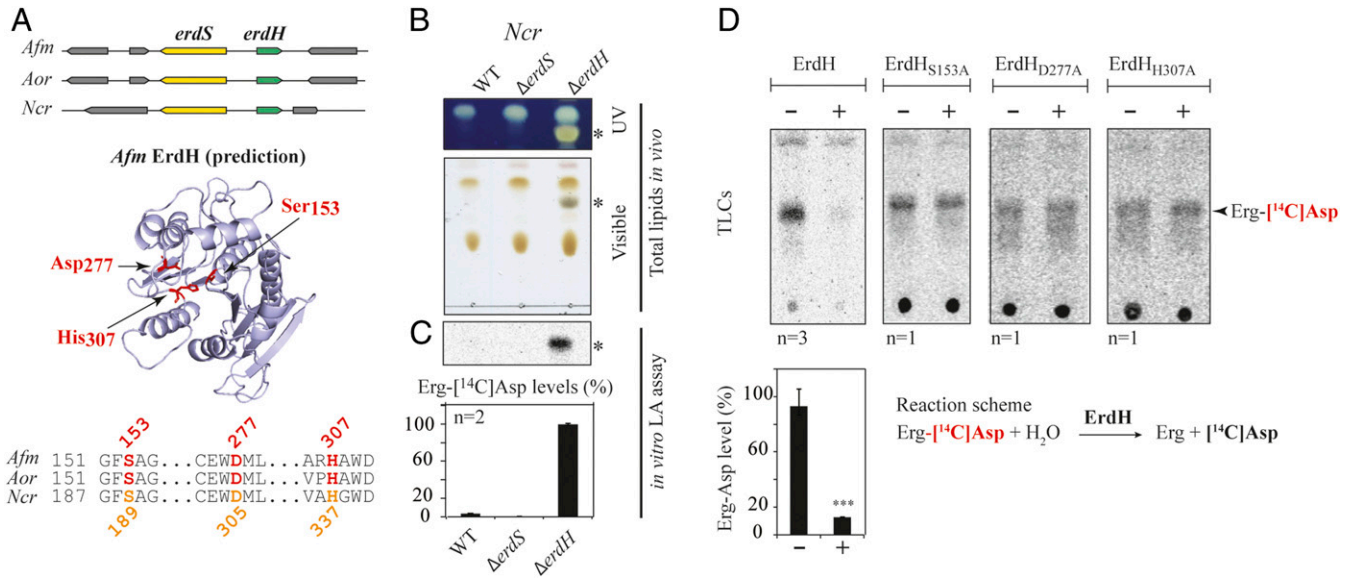

Fig. 5. Detection and characterization of ErdH in fungi carrying ErdS. (*A*) Schematic representation of the genomic context of the *erdS* (yellow) and *erdH* (for Erg-Asp hydrolase, in green) genes locus from *Afm*, *Aor*, and *Ncr* that highlights that *erdS* and *erdH* are found in a divergent orientation. Phyre2-based α/β-hydrolase–like predicted structure of *Afm* ErdH and active site alignments of *Afm*, *Aor*, and *Ncr* ErdHs. Ser-Asp-His catalytic triads of α/β-hydrolases/lipases (S153, D277, and H307 in *Afm* ErdH) are displayed and highlighted on the structure prediction and the alignment. (*B*) Total lipids from WT, Δ*erdS*, and Δ*erdH Ncr* strains were separated by TLC and stained with sulfuric acid/$MnCl_2$ and observed under UV or visible light (n = 3); * indicates Erg-Asp. (*C*) In vitro measurements of Erg-[^{14}C]Asp synthesis by LA assay using protein extracts from the WT, Δ*erdS*, and Δ*erdH Ncr* strain protein extracts, using pure *Sce* $tRNA^{Asp}$ as a substrate (n = 2). (*D*) In vitro measurement of the Erg-[^{14}C]Asp hydrolase activities of purified recombinant WT (n = 3) or catalytic mutant *Ncr* ErdHs (n = 1). (*C* and *D*) The Student's *t* test was used to determine significance of the means of the data; ***P < 0.005.

Downloaded by guest on September 16, 2020

proteins, with 780 (77%) being ErdS with a minimal length of ~800 aa (no N- or C-terminal extensions) and a maximal length of 1,417 aa (with long N- and/or C-terminal appendages). "Standalone" DUF2156 domains (23%) were also detected and often accounted for ErdS forms with either the AspRS or the DUF2156 domain truncated. A closer look at the phylogenomic distribution of complete ErdS (AspRS-DUF2156 fusions) highlighted that they are present only in "higher" fungi (Dikarya, both Ascomycota and Basidiomycota), and specifically among 9 out of the 13 fungal lineages analyzed (Fig. 6*A*), with the notable exception of Saccharomycotina (including *Sce*), Lecanoromycetes, and Pezizomycetes. ErdS is present in prominent human pathogens such as *Afm* (20), *Histoplasma capsulatum*, or *Cryptococcus neoformans* (*Cne*), plant pathogens such as *Fusarium oxysporum*, *Magnaporthe oryzae*, or *Ustilago maydis*, insect pathogens like *Beauveria bassiana* or *Metarhizium* spp., and also fungi of biotechnological interest like *Aor* or *Ncr*. We then visualized the synteny of the *erdS* gene in various fungi and observed that, in most of the cases, the *erdH* gene was almost always present next to *erdS* with the same divergent orientation in numerous species, showing that the linkage between the two genes is conserved. In fungi lacking *erdS*, the *erdH* genes were also absent, as judged from the absence of proteins with significant sequence homology to ErdH (Fig. 6*A*). Overall, the whole ErdS/ErdH enzymatic pathway seemed conserved across "higher" fungi.

Finally, in order to confirm that Erg-Asp is synthesized in several representative ErdS/ErdH-containing fungi, we extracted and analyzed, by TLC, total lipids from a collection of 15 fungal species (13 Ascomycota and 2 Basidiomycota). As expected from the absence of an *erdS* gene, Erg-Asp was absent in the four tested Saccharomycotina. However, it was detected in eight Ascomycota and one Basidiomycota species tested (Fig. 6*B*). The only exceptions were *Ncr* (Ascomycota), as already explained above, and *Cne* (Basidiomycota), for which the *erdS* gene regulation and/or the activity of ErdH could also account for the absence of Erg-Asp. Taken together, our results confirm that Erg-Asp is likely widely distributed and conserved across fungi.

Discussion

A wide range of bacteria possess membrane proteins with an AAT activity, namely MprFs, that reroute aa-tRNAs from protein synthesis to cell surface remodeling, thereby intensifying antimicrobial resistance, pathogenicity, and/or virulence (4, 7,

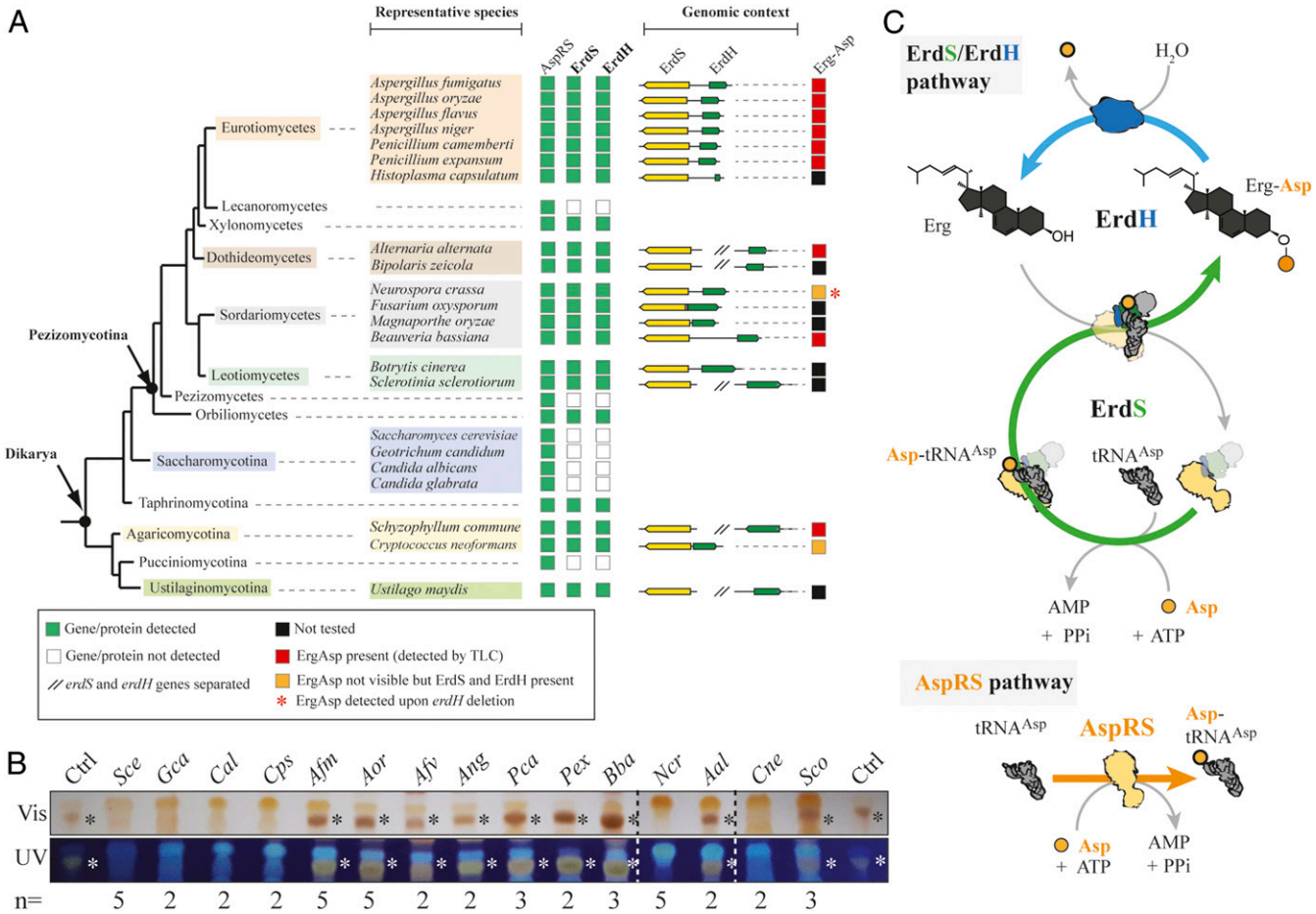

Fig. 6. The Erg-Asp lipid metabolic enzymes ErdS and ErdH are conserved across "higher" fungi. (*A*) The presence (green square) or absence (white squares) of a regular AspRS, ErdS (yellow), or ErdH (green) genes across fungal species is indicated, and the organization of the locus is shown; // indicates that *erdS* and *erdH* genes are interspaced. (*B*) TLC-based analysis of total lipids extracted from 15 species among the representative ones displayed in *A*. The TLC plates (number of replicates indicated for each strain) stained with sulfuric acid/$MnCl_2$ solution and observed under white (Vis) or UV light were cropped to the area of interest; * indicates Erg-Asp synthesis (red squares in *A*) as revealed by the detection of a dark brown band with mobility equivalent to control Erg-Asp. *Gca*: *Geotrichum candidum*; *Cal*: *Candida albicans*; *Cps*: *Candida parapsilosis*; *Afv*: *Aspergillus flavus*; *Ang*: *Aspergillus niger*; *Pca*: *Penicillium camemberti*; *Pex*: *Penicillium expansum*; *Bba*: *Beauveria bassiana*; *Aal*: *Alternaria alternata*; *Sco*: *Schizophyllum commune*. (*C*) A schematic model representing the turnover between Erg-Asp synthesis, and hydrolysis. The green arrow shows ErdS activities (Asp-$tRNA^{Asp}$ production and Asp modification of Erg), and the blue arrow indicates the ErdH-dependent hydrolysis of Erg-Asp. All ErdS-containing fungi always possess a canonical AspRS to ensure Asp-$tRNA^{Asp}$ production for protein synthesis (AspRS pathway).

Downloaded by guest on September 16, 2020

11). Our work reveals that most of the fungal species found within the Dikarya subkingdom possess bifunctional enzymes, ErdS, that use ATP, L-Asp, and $tRNA^{Asp}$ to produce Asp-$tRNA^{Asp}$ in the AspRS domain, this latter product being used in a second step by the appended DUF2156/Asp-tRNA transferase module to transfer Asp from its $tRNA^{Asp}$ onto the 3β-OH group of Erg, yielding a novel form of conjugated sterol, Erg-Asp (Fig. 6*C*). Erg-Asp synthesis constitutes a change of paradigm for three main reasons: 1) this is a tRNA-dependent lipid modification process in eukaryotes; 2) the use of Asp as a lipid modifier, that has no equivalent in bacteria, and 3) the modification of Erg (instead of glycerolipids) with an aa that had, to our knowledge, never been described, despite the widespread distribution of Erg-Asp synthesis in fungi (Fig. 6*B*). Moreover, we found no evidence in the literature or databases of any 3β-*O*-aminoacylated sterols. Erg-Asp likely escaped previous detection because, as an ester, most of alkaline extraction procedures used for sterols extraction promote its hydrolysis. Erg-Asp is therefore a novel type of sterol conjugate, specific to fungi, that is performed by ErdSs enzymes, through a tRNA-dependent process. It is worth noting that the fusion of the AspRS and the transferase (DUF2156) domain is required for full activity, since the standalone DUF2156 domain was poorly active in the *Sce* heterologous model (Fig. 3*B*) or inactive in *Aor* (Fig. 2*C*). Channeling of Asp-$tRNA^{Asp}$ from the AspRS to the appended DUF2156 is the most plausible explanation. It would explain the better capacity of the AspRS domain alone, that releases Asp-$tRNA^{Asp}$, to complement the *Sce* Δ*dps1* strain over the full-length ErdS (*SI Appendix*, Fig. S4*A*), that transfers Asp-$tRNA^{Asp}$ directly to the transferase domain for sterol aspartylation, likely without releasing it frequently. Of note is that all fungal species that encode ErdS also possess a regular cytoplasmic AspRS (Fig. 6*A* and *SI Appendix*, Fig. S1*A*), suggesting that the Asp-$tRNA^{Asp}$ generated by the AspRS moiety of ErdS is probably entirely dedicated to lipid modification, thereby necessitating a second AspRS to produce the Asp-$tRNA^{Asp}$ used for translation, as observed in all inspected fungi (Fig. 6 *A* and *C* and *SI Appendix*, Fig. S1*A*).

Characterization of ErdH, that hydrolyzes Erg-Asp in fungi, revealed that, like in bacteria, ErdS-containing fungi possess a homeostasis system that enables the tRNA-dependent aminoacylation of a lipid (ErdS) and its deacylation through hydrolysis (ErdH), suggesting that Erg-Asp levels might be tightly controlled. This provides an explanation for the apparent absence of Erg-Asp in total lipids from *Ncr* or *Cne* (Figs. 5*B* and 6*B*) under the growth conditions used. Of note is that this turnover cycle recalls that of the acyl-CoA transferase-dependent fatty acylation and lipase-dependent deacylation systems involved in sterols storage, turnover, and trafficking in eukaryotes, including fungi (21). The *erdS* and *erdH* genes tend to cluster as divergently expressed units within the same genomic locus, which resembles the cluster organization of genes with metabolically related functions found in many fungi (22). This suggests that *erdS* and *erdH* may be coregulated at the transcriptional level, likely to control the balance between Erg and Erg-Asp, a tempting hypothesis that remains to be analyzed. Erg-Asp levels could also depend on the turnover (expression and degradation) and regulation (posttranslational modifications, etc.) of ErdS and ErdH and/or on the relative subcellular localization of both enzymes. Such potential species-specific spatiotemporal regulations of Erg-Asp homeostasis could account for the different steady-state levels of Erg-Asp that we observed between the various fungal species, especially between *Aspergillus* spp. and *Ncr*. We have not been able, so far, to identify the subcellular localization of either ErdS or ErdH. Bioinformatics predictions (Wolf PSort, MitoProt II software), however, suggest that ErdH might be mitochondrial in *Aspergillus* spp., while ErdS is predicted to be cytoplasmic and/or nucleocytoplasmic, a fact that is not unusual for aaRSs (23). Also, no plausible membrane-spanning or membrane-anchoring helices could be predicted in ErdS or ErdH, which differs from bacterial homologs: MprFs have N-terminal membrane-spanning domains, and aminoacyl-glycerolipid hydrolases have N-terminal secretion signals to ensure correct periplasmic or extracellular localization (4). Very preliminary subcellular fractionation experiments suggest that, in *Afm* or in the heterologous model *Sce*, ErdS is not soluble but is associated with membranes, but the nature of those membranes remains unknown. Of note, in any case, is that membrane association of ErdS—to recognize Erg—requires that the enzyme be exposed to the cytoplasmic space, where its $tRNA^{Asp}$, Asp, and ATP substrates are present (*SI Appendix*, Fig. S8).

Erg is the major sterol found in fungal plasma membranes (24). Its function is analogous to that of Cho in mammals, which includes modulating permeability and fluidity of the lipid bilayer (25, 26) and regulating the activity of membrane proteins, such as G protein-coupled receptors (27) or V-ATPases (28). Erg, together with sphingolipids, regulates membrane trafficking, which is illustrated in filamentous species, such as *Aspergillus* spp., by a constant supply of Erg at the tip of mycelia to form lipid microdomains that are crucial to polarized cell growth (29). Erg also plays multiple roles in pathogenicity and in antifungal resistance (24, 30, 31). Incidentally, because Erg biosynthesis pathway differs from that found in humans for Cho, it is one of the main targets of current antifungal drugs (32).

Although we deciphered the function of ErdS and ErdH, the role of Erg-Asp in the biology of fungi now remains to be discovered, and this will be the focus of our future work. The viability of the Δ*erdS* strains of *Afm*, *Aor*, and *Ncr* shows that neither ErdS nor ErdH are essential under standard growth conditions. However, as discussed below, this fact does not exclude functions that could become essential or contribute to the overall fitness of fungi under challenging conditions, such as in the presence of membrane-targeting antifungals or antimicrobial peptides, which may explain the evolutionary conservation of the enzymatic system across Dikarya. As a first hypothesis, aspartylation of Erg by ErdS might play a role similar to aminoacylated glycerolipids in bacteria, regarding antimicrobial resistance (4, 7, 11, 32). Indeed, addition of L-Asp on the neutral and highly hydrophobic Erg leads to a novel zwitterionic sterol, which may significantly change Erg physicochemical properties within membranes, by influencing its phase behavior, its lateral diffusion, and/or its interaction with other lipids. Local Erg-Asp synthesis might, in turn, influence membranes' overall properties such as interface hydration, membrane proteins composition, permeability, and/or fluidity, or the activity and/or localization of membrane proteins. Therefore, Erg-Asp could participate in membrane remodeling processes that might have an impact on antifungal resistance, notably, in the case of polyenes, known to directly interact with Erg to form pores, since aspartylation of the 3β-OH could change their interactions with Erg (33), a hypothesis that we will explore. Erg-Asp levels (7 to 20% of free Erg in *Aor*; *SI Appendix*, Fig. S9) upon growth in rich medium seem incompatible with an overall surface remodeling; however, nothing is currently known on the regulation of Erg-Asp synthesis and the amount of modification that can occur under challenging conditions. As an illustration, in *Sce*, an Erg acetylation/deacylation cycle, that functionally resembles our ErdS/ErdH enzymatic system, involves the Atf2 acetyltransferase and the Say1 esterase. This nonessential enzymatic system protects cells from the accumulation of toxic Erg intermediates within membranes, and from the effect of membrane-disrupting agents such as the antifungal agent eugenol (34), suggesting that the ErdS/ErdH system and Erg aspartylation might be of importance in resistance when Erg biosynthesis inhibitors, such as azole derivatives, that trigger accumulation of toxic Erg intermediates, are used against fungi. This could be tested by determining the susceptibility of WT (Erg-Asp-containing), Δ*erdS* (Erg-Asp-deficient), Δ*erdH* (Erg-Asp-accumulating),

Downloaded by guest on September 16, 2020

or overexpressing (Erg-Asp-overproducing) strains in the presence of azole derivatives.

While lipid modifications are usually involved in cells' surface remodeling and antimicrobial resistance in bacteria (7, 35), they also often participate in membrane trafficking and lipid-derived signaling in eukaryotes (3), like, for example, in the case of phosphoinositides or sphingolipids (36). Erg-Asp is produced at levels (7 to 20% of free Erg in *Aor*; *SI Appendix*, Fig. S9) that could be compatible with such cellular functions. Ergosteryl-3β-*O*-glucoside (Erg-Glc), another sterol conjugate, produced by Erg glycosylation, is nonessential, but known to actively participate in the regulation of autophagy in several yeasts and in *Aor* (37, 38), likely through the recruitment of protein partners on membrane structures (39). It is therefore possible that Erg aspartylation could intervene in the recruitment of protein factors on membranes (Erg-containing microdomains, etc.) and influence regulatory or trafficking pathways. Finally, bacterial esterases that remove aa modifications from glycerolipids also influence virulence in *A. tumefaciens* (10). Those observations in various bacterial lipid aminoacylation systems or fungal sterol modification pathways raise the question of the contribution of Erg aspartylation and deacylation to those processes in fungi. Given the conservation of the ErdS/ErdH enzymatic system across Dikarya, these aspects will now have to be addressed experimentally to decipher the function of Erg-Asp.

Materials and Methods

Materials, Strains, and Growth Condition. The *erdS* codon-optimized synthetic gene was purchased from the Genscript Corporation. The anti-DUF2156 polyclonal antibody production was performed by Covalab (R&D in Biotechnology). Some of the fungal strains were ordered from the Fungal Genetics Stock Center. The CEA17 Δ*akuB*^{KU80} strain of *Afm* (40) and the RIB40 strain of *Aor* (41) have been used as parental strain for this study. The routine growth and maintenance of *Afm* and *Aor* are described in *SI Appendix, Supplementary Materials and Methods*. The strains (bacterial and fungi) used in this study are listed in *SI Appendix*, Table S1.

Total Lipid Extraction from *Sce* and from Filamentous Fungi. Lipid extraction protocols for *Sce* and filamentous fungi were adapted from the Bligh and Dyer procedure (42). Briefly, *Sce* strains were grown in synthetic complete (SC) medium without leucine (SC-LEU) (MP Biomedicals) until optical density 600 nm ($OD_{600\ nm}$) reached 1.0. An equivalent of 150 $OD_{600\ nm}$ of *Sce* cells were centrifuged at 4,000 × *g* for 15 min at 4 °C. The cell pellet was resuspended in 1 mL of Na-acetate 120 mM pH 4.5. Mechanical cell disruption was performed in a FastPrep-24 apparatus (MP Biomedicals, serial no. 10020698) in the presence of 400 μL of glass beads (ø 0.25 mm to 0.5 mm, Roth) at 6 m/s, for 1 min repeated 6 times, with cooling on ice between each step; 3.75 vol of MeOH:$CHCl_3$ 2:1 (v:v) were added, and the mixture was incubated on a rotating wheel at 4 °C for 3 h. Then, 1.25 vol of $CHCl_3$ and Na-acetate 120 mM pH 4.5 were successively added and mixed by vortexing. The mixture was then centrifuged at 4,000 × *g*, 4 °C for 10 min to obtain two phases. The lower organic phase, containing the lipids, was transferred into a new tube, dried under vacuum, and stored at −20 °C until use or resuspended in 50 μL to 200 μL of MeOH:$CHCl_3$ 1:1 (vol/vol) for analysis by TLC.

For filamentous fungi, the same protocol was applied on 2 g of mycelia that were ground in a mortar with a pestle in liquid nitrogen to obtain a fine powder. Furthermore, the incubation on the rotating wheel was performed overnight at 4 °C.

Lipid X Purification. LX was purified from adaptation of the flash chromatography procedure used for bacterial aminoacylated lipids (11). Total lipids extracted from 500 $OD_{600\ nm}$ of *Sce* cells were solubilized in 200 μL of chloroform and loaded on a 1.5-mL silica gel (Sigma-Aldrich, pore size 60) glass column preequilibrated with $CHCl_3$. After absorption of lipids on the column, nonpolar lipids and glycolipids were eluted with 10 mL of chloroform followed by 10 mL of acetone, respectively. To elute polar lipids, various ratios of $CHCl_3$:MeOH from 9:1 to 6:4 (vol/vol) (20 mL each) were used, and elution fractions were collected in 2-mL samples in glass tubes. Fractions were dried under vacuum, resolubilized in 35 μL of MeOH:$CHCl_3$ (1:1, vol/vol), and visualized by TLC.

TLC Analyses. Dried lipid samples were resuspended in MeOH:$CHCl_3$ (1:1, vol/vol) and spotted onto 10 × 20 cm silica gel on TLC Al foils (Sigma-Aldrich). TLC was developed with a $CHCl_3$:MeOH:H_2O (130:50:8 vol/vol/vol) mobile phase (10 min at room temperature [RT]), and plates were stained with either $MnCl_2$/sulphuric acid or ninhydrin or bromocresol green. $MnCl_2$/sulphuric acid, a universal staining (43), was prepared with 0.8 g of $MnCl_2$ tetrahydrate dissolved in 240 mL of 50% (vol/vol) MeOH supplemented with 9 mL of concentrated sulphuric acid. To detect primary amines (pink color), ninhydrin 0.4% (wt/vol) (Sigma-Aldrich) was used. To reveal carboxylate-containing compounds (blue color) with a pK_a below 5.0 (44), bromocresol green (0.04 g) (Sigma-Aldrich) dissolved in absolute ethanol and NaOH 0.1 M was used. In the case of $MnCl_2$/sulphuric acid and ninhydrin stains, plates were heated at 100 °C until coloration developed, while direct ultraviolet (UV) (254 or 315 nm) visualization was performed with bromocresol green. Quantification of LX (Erg-Asp), PE, or PG spots was performed using the ImageJ software. Lipid spots signals (number of pixels, *N*) were normalized to that of PE (N_{LX}/N_{PE}). In the absence of LX (Erg-Asp), PG becomes visible at the same position; the PG/PE signal thus represents the background signal in the absence of LX.

MS Analyses. Analyses of total purified lipid extracts were performed on a liquid chromatograph Surveyor Plus with an autosampler and coupled with an LTQ-XL ion trapanalyzer (Thermo Finnigan). Ten microliters of filtered lipid extracts were injected on a Cogent Diamond Hydride (250 × 4.6 mm, 4 μm, Microsolv) at a temperature of 40 °C as described in ref. 45 with minor modifications. Briefly, elution was performed at a flow rate of 1 mL/min in hydrophilic interaction liquid chromatography (HILIC) conditions with a binary gradient running from 99.7:0.3 (A:B) to 75:25 in 40 min, where A was acetonitrile and B was 40 mM aqueous ammonium formate. Both solutions contained 5.5 mM formic acid. The instrument was tuned by direct infusion of cholesterol (Avanti) in positive mode. Drying gas flow rate was 20 units, and temperature of the ESI was 380 °C. Full-scan spectra were collected in the 110 to 2,000 *m/z* range, and data-dependent Zoom and MS2 spectra were acquired on the 15 most intense peaks. Data were analyzed with XcaliburQual Browser.

In Vitro LA Assay. Prior to lipid aminoacylation, the in vitro $tRNA^{Asp}$ aspartylation was performed as described in *SI Appendix, Supplementary Materials and Methods*. Lipid or sterols aspartylation assays were adapted from lipid aminoacylation protocols used for bacterial MprFs (42). Briefly, reactions were performed in the following aminoacylation mix: Na-Hepes 100 mM pH 7.2 buffer containing KCl 30 mM, $MgCl_2$ 12 mM, ATP 10 mM, bovine serum albumin 0.1 mg/mL, pure yeast $tRNA^{Asp}$ (10 μM) (46), [U-^{14}C]-Asp (280 cpm/pmol, Perkin-Elmer, NEC268E050UC) in a final volume of 50 μL. To test the transfer of [^{14}C]-Asp onto lipids, total lipids were added to a final concentration of 2 mg/mL, and commercial pure sterols (Erg and Cho) were added to a final concentration of 0.5 mg/mL. When [^{3}H]-Erg (10 Ci/mmol, Hartmann Analytic) was used, 20,000 cpm were added to the reaction mix. The resulting suspension was sonicated for 30 s in a sonicator bath at RT, and the enzyme (0.1 to 0.5 μg) or crude extracts of *Afm*, *Aor*, or *Ncr* (20 μg total proteins) were added to initiate the reaction before a 40-min-long incubation at 30 °C (1 h for crude extracts). To test the tRNA dependency of the reaction, 1 μg of RNase A from bovine pancreas was added 10 min before initiation of the reaction.

After incubation, reactions were stopped with addition of 500 μL of $CHCl_3$:MeOH:Na-acetate 120 mM pH 4.5 (130:50:8, vol/vol/v) and vortexing. Then, 130 μL of $CHCl_3$ and 130 μL of Na-acetate 120 mM pH 4.5 were successively added, and the mixture was vortexed and centrifuged for 1 min at 5,000 × *g* (RT). The lower organic phase was recovered and dried under vacuum. Reaction products were dissolved in a $CHCl_3$:MeOH (1:1, v:v) mixture, spotted on TLC plates, and separated with the $CHCl_3$:MeOH:H_2O mobile phase. TLC plates were exposed onto an imaging plate (Fuji Imaging plate) for at least 2 h. Radioactivity was detected using a Typhoon TRIO variable Mode Imager (GE Healthcare). Quantification of LX (Erg-Asp) radioactive spots was performed using the ImageJ software (number of pixels).

In Vitro Lipid Deacylation Assay. To generate Erg-[^{14}C]-Asp, we used the protocol described above for LA assay. RNase A was added and incubated for 20 min at 30 °C to hydrolyze $tRNA^{Asp}$ and stop the tRNA-dependent aspartylation catalyzed by ErdS. Then, 0.1 μM of purified recombinant ErdH or ErdH variants were added, and the reaction mixture was incubated for 30 min at 30 °C. Lipids were extracted with the Bligh and Dyer procedure as described above, dried, resuspended in $CHCl_3$:MeOH (1:1, vol/vol), and analyzed on TLC with the $CHCl_3$:MeOH:H_2O (130:50:8, v:v:v) solvent, and results were analyzed by phosphorimaging as described above.

Downloaded by guest on September 16, 2020

Statistical Analyses. The Student's *t* test was used to determine significance of the means of the data.

Materials and Data Availability. All available data are already included in the manuscript. All materials and strains are freely available (contact: h.becker@unistra.fr; frfischer@unistra.fr).

ACKNOWLEDGMENTS. This work was supported by the Fondation pour la Recherche Médicale (FRM), to H.D.B. (Grant DBF20160635713), by "Mito-Cross" Laboratory of Excellence (Grant ANR-10-IDEX-0002-02 to H.D.B.), by the University of Strasbourg (to H.D.B.), by an IDEX from the University of Strasbourg (W17RAT81, to F.F.), the National Center for Scientific Research (H.D.B, B.S., F.F., and N.Y.), and the Meiji University (T.K., Y.S., S.T., D.Y., and H.N.). N.Y. was supported by a fellowship from the French Ministère de l'Enseignement Supérieur et de la Recherche, and N.M. was supported by a postdoctoral fellowship from the FRM (Grant DBF20160635713). H.R. and C.D.G. were supported by NIH Grant 1R21AI144481-01. We thank J.-P.L., Dr. I. Mouyna, Dr. A. Beauvais, and Dr. T. Fontaine (Institut Pasteur, Paris, France) for providing *A. fumigatus* strains and deletion cassette templates, for having trained F.F. on the manipulation of the strains, and for thoughtful discussions. We thank H.N. for *A. oryzae* strains and related plasmids and Maryline Brock (University of Strasbourg) for other fungal species. In addition, we thank Dr. Sylvie Friant for critical review, experimental suggestions, and careful reading of the manuscript.

1. O. Bohuszewicz, J. Liu, H. H. Low, Membrane remodelling in bacteria. *J. Struct. Biol.* **196**, 3–14 (2016).
2. E. M. Fozo, E. A. Rucks, The making and taking of lipids: The role of bacterial lipid synthesis and the harnessing of host lipids in bacterial pathogenesis. *Adv. Microb. Physiol.* **69**, 51–155 (2016).
3. A. Singh, M. Del Poeta, Lipid signalling in pathogenic fungi. *Cell. Microbiol.* **13**, 177–185 (2011).
4. R. N. Fields, H. Roy, Deciphering the tRNA-dependent lipid aminoacylation systems in bacteria: Novel components and structural advances. *RNA Biol.* **15**, 480–491 (2018).
5. M. Ibba, D. Soll, Aminoacyl-tRNA synthesis. *Annu. Rev. Biochem.* **69**, 617–650 (2000).
6. S. Hebecker *et al*., Structures of two bacterial resistance factors mediating tRNA-dependent aminoacylation of phosphatidylglycerol with lysine or alanine. *Proc. Natl. Acad. Sci. U.S.A.* **112**, 10691–10696 (2015).
7. C. Slavetinsky, S. Kuhn, A. Peschel, Bacterial aminoacyl phospholipids–Biosynthesis and role in basic cellular processes and pathogenicity. *Biochim. Biophys. Acta Mol. Cell Biol. Lipids* **1862**, 1310–1318 (2017).
8. W. Arendt, M. K. Groenewold, S. Hebecker, J. S. Dickschat, J. Moser, Identification and characterization of a periplasmic aminoacyl-phosphatidylglycerol hydrolase responsible for *Pseudomonas aeruginosa* lipid homeostasis. *J. Biol. Chem.* **288**, 24717–24730 (2013).
9. A. M. Smith, J. S. Harrison, K. M. Sprague, H. Roy, A conserved hydrolase responsible for the cleavage of aminoacylphosphatidylglycerol in the membrane of *Enterococcus faecium*. *J. Biol. Chem.* **288**, 22768–22776 (2013).
10. M. K. Groenewold *et al*., Virulence of *Agrobacterium tumefaciens* requires lipid homeostasis mediated by the lysyl-phosphatidylglycerol hydrolase AcvB. *Mol. Microbiol.* **111**, 269–286 (2019).
11. A. M. Smith *et al*., tRNA-dependent alanylation of diacylglycerol and phosphatidylglycerol in *Corynebacterium glutamicum*. *Mol. Microbiol.* **98**, 681–693 (2015).
12. M. Datt, A. Sharma, Novel and unique domains in aminoacyl-tRNA synthetases from human fungal pathogens *Aspergillus niger*, *Candida albicans* and *Cryptococcus neoformans*. *BMC Genomics* **15**, 1069 (2014).
13. M. Ruff *et al*., Class II aminoacyl transfer RNA synthetases: Crystal structure of yeast aspartyl-tRNA synthetase complexed with tRNA(Asp). *Science* **252**, 1682–1689 (1991).
14. L. Klug, G. Daum, Yeast lipid metabolism at a glance. *FEMS Yeast Res.* **14**, 369–388 (2014).
15. L. Ador *et al*., Active site mapping of yeast aspartyl-tRNA synthetase by in vivo selection of enzyme mutations lethal for cell growth. *J. Mol. Biol.* **288**, 231–242 (1999).
16. J. Cavarelli *et al*., The active site of yeast aspartyl-tRNA synthetase: Structural and functional aspects of the aminoacylation reaction. *EMBO J.* **13**, 327–337 (1994).
17. J. V. Headley, K. M. Peru, B. Verma, R. D. Robarts, Mass spectrometric determination of ergosterol in a prairie natural wetland. *J. Chromatogr. A* **958**, 149–156 (2002).
18. H. V. Colot *et al*., A high-throughput gene knockout procedure for *Neurospora* reveals functions for multiple transcription factors. *Proc. Natl. Acad. Sci. U.S.A.* **103**, 10352–10357 (2006).
19. K. McCluskey, A. Wiest, M. Plamann, The fungal genetics Stock center: A repository for 50 years of fungal genetics research. *J. Biosci.* **35**, 119–126 (2010).
20. A. Abad *et al*., What makes *Aspergillus fumigatus* a successful pathogen? Genes and molecules involved in invasive aspergillosis. *Rev. Iberoam. Micol.* **27**, 155–182 (2010).
21. N. Jacquier, R. Schneiter, Mechanisms of sterol uptake and transport in yeast. *J. Steroid Biochem. Mol. Biol.* **129**, 70–78 (2012).
22. H. W. Nützmann, C. Scazzocchio, A. Osbourn, Metabolic gene clusters in eukaryotes. *Annu. Rev. Genet.* **52**, 159–183 (2018).
23. S. Debard *et al*., Nonconventional localizations of cytosolic aminoacyl-tRNA synthetases in yeast and human cells. *Methods* **113**, 91–104 (2017).
24. M. L. Rodrigues, The multifunctional fungal ergosterol. *MBio* **9**, e01755-18 (2018).
25. L. M. Douglas, J. B. Konopka, Fungal membrane organization: The eisosome concept. *Annu. Rev. Microbiol.* **68**, 377–393 (2014).
26. M. Kodedová, H. Sychrová, Changes in the sterol composition of the plasma membrane affect membrane potential, salt tolerance and the activity of multidrug resistance pumps in *Saccharomyces cerevisiae*. *PLoS One* **10**, e0139306 (2015).
27. S. Morioka *et al*., Effect of sterol composition on the activity of the yeast G-protein-coupled receptor Ste2. *Appl. Microbiol. Biotechnol.* **97**, 4013–4020 (2013).
28. Y. Q. Zhang *et al*., Requirement for ergosterol in V-ATPase function underlies antifungal activity of azole drugs. *PLoS Pathog.* **6**, e1000939 (2010).
29. R. Fischer, N. Zekert, N. Takeshita, Polarized growth in fungi—Interplay between the cytoskeleton, positional markers and membrane domains. *Mol. Microbiol.* **68**, 813–826 (2008).
30. L. Alcazar-Fuoli, E. Mellado, Ergosterol biosynthesis in *Aspergillus fumigatus*: Its relevance as an antifungal target and role in antifungal drug resistance. *Front. Microbiol.* **3**, 439 (2013).
31. K. Koselny *et al*., A genome-wide screen of deletion mutants in the filamentous Saccharomyces cerevisiae background identifies ergosterol as a direct trigger of macrophage pyroptosis. *MBio* **9**, e01204-18 (2018).
32. T. K. Mazu, B. A. Bricker, H. Flores-Rozas, S. Y. Ablordeppey, The mechanistic targets of antifungal agents: An overview. *Mini Rev. Med. Chem.* **16**, 555–578 (2016).
33. D. M. Kamiński, Recent progress in the study of the interactions of amphotericin B with cholesterol and ergosterol in lipid environments. *Eur. Biophys. J.* **43**, 453–467 (2014).
34. R. Tiwari, R. Köffel, R. Schneiter, An acetylation/deacetylation cycle controls the export of sterols and steroids from S. cerevisiae. *EMBO J.* **26**, 5109–5119 (2007).
35. R. Nuri, T. Shprung, Y. Shai, Defensive remodeling: How bacterial surface properties and biofilm formation promote resistance to antimicrobial peptides. *Biochim. Biophys. Acta* **1848**, 3089–3100 (2015).
36. J. O. De Craene, D. L. Bertazzi, S. Bär, S. Friant, Phosphoinositides, major actors in membrane trafficking and lipid signaling pathways. *Int. J. Mol. Sci.* **18**, 634 (2017).
37. S. Grille, A. Zaslawski, S. Thiele, J. Plat, D. Warnecke, The functions of steryl glycosides come to those who wait: Recent advances in plants, fungi, bacteria and animals. *Prog. Lipid Res.* **49**, 262–288 (2010).
38. T. Kikuma, T. Tadokoro, J. I. Maruyama, K. Kitamoto, AoAtg26, a putative sterol glucosyltransferase, is required for autophagic degradation of peroxisomes, mitochondria, and nuclei in the filamentous fungus *Aspergillus oryzae*. *Biosci. Biotechnol. Biochem.* **81**, 384–395 (2017).
39. S. Yamashita, M. Oku, Y. Sakai, Functions of PI4P and sterol glucoside are necessary for the synthesis of a nascent membrane structure during pexophagy. *Autophagy* **3**, 35–37 (2007).
40. M. E. da Silva Ferreira *et al*., The akuB(KU80) mutant deficient for nonhomologous end joining is a powerful tool for analyzing pathogenicity in *Aspergillus fumigatus*. *Eukaryot. Cell* **5**, 207–211 (2006).
41. M. Machida *et al*., Genome sequencing and analysis of *Aspergillus oryzae*. *Nature* **438**, 1157–1161 (2005).
42. H. Roy, M. Ibba, Monitoring Lys-tRNA(Lys) phosphatidylglycerol transferase activity. *Methods* **44**, 164–169 (2008).
43. S. K. Goswami, C. F. Frey, Manganous chloride spray reagent for cholesterol and bile acids on thin-layer chromatograms. *J. Chromatogr. A* **53**, 389–390 (1970).
44. A. Shokrollahi, F. Firoozbakht, Determination of the acidity constants of neutral red and bromocresol green by solution scanometric method and comparison with spectrophotometric results. *Beni. Suef Univ. J. Basic Appl. Sci.* **5**, 13–20 (2016).
45. E. Cífková, R. Hájek, M. Lísa, M. Holčapek, Hydrophilic interaction liquid chromatography-mass spectrometry of (lyso)phosphatidic acids, (lyso)phosphatidylserines and other lipid classes. *J. Chromatogr. A* **1439**, 65–73 (2016).
46. G. Keith, J. Gangloff, G. Dirheimer, Isolement des tRNATyr et tRNAAsp de levure de bière hautement purifiés. *Biochimie* **53**, 123–125 (1971).

Downloaded by guest on September 16, 2020

Supporting Information

Supplemental Figures

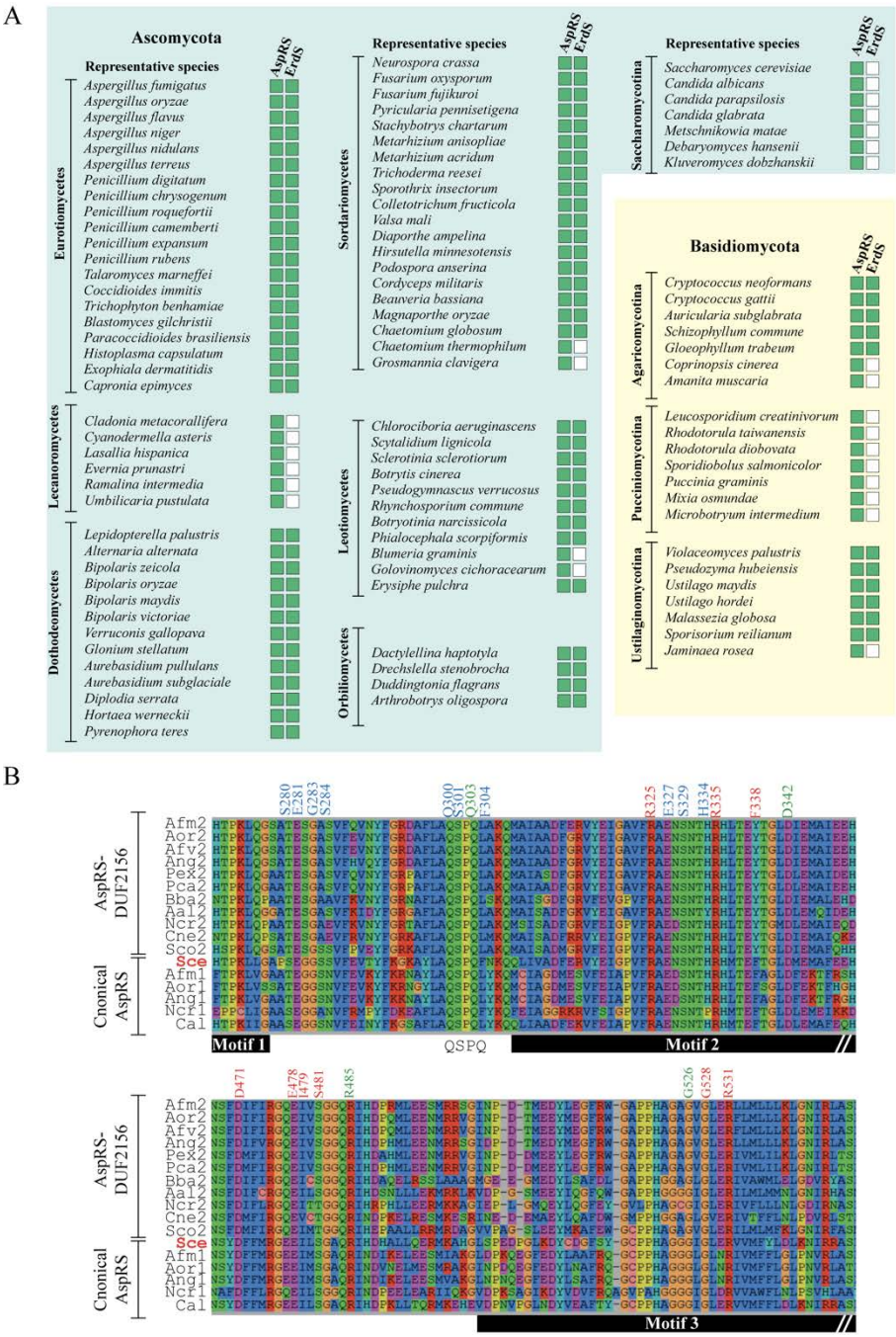

Figure S1: (**A**) Distribution in representative species of each class of Dikarya of the presence (green box) or absence (white box) of a canonical AspRS and ErdS. (**B**) Conservation of the consensus class II aaRS motifs 1, 2 and 3 in the alignment of 11 ErdS (AspRS-DUF2156) and 6 canonical AspRSs. *Afm: Aspergillus fumigatus, Aor: Aspergillus oryzae, Afv: Aspergillus flavus, Ang: Aspergillus niger, Pex: Penicillium expansum, Pca: Penicillium camemberti, Bba:*

www.pnas.org/cgi/doi/10.1073/pnas.2003266117

Beauveria bassiana, Aal: Alternaria alternata, Ncr: Neurospora crassa, Cne: Cryptococcus neoformans, Sco: Schizophyllum commune, Sce: Saccharomyces cerevisiae, Cal: Candida albicans. Numberings are indicated relative to the *Sce* AspRS sequence. Residues involved in the recognition of ATP, and aspartate are indicated in red and green respectively, whereas residues responsible for the $tRNA^{Asp}$acceptor arm recognition through its 3'-CCA are indicated in blue.

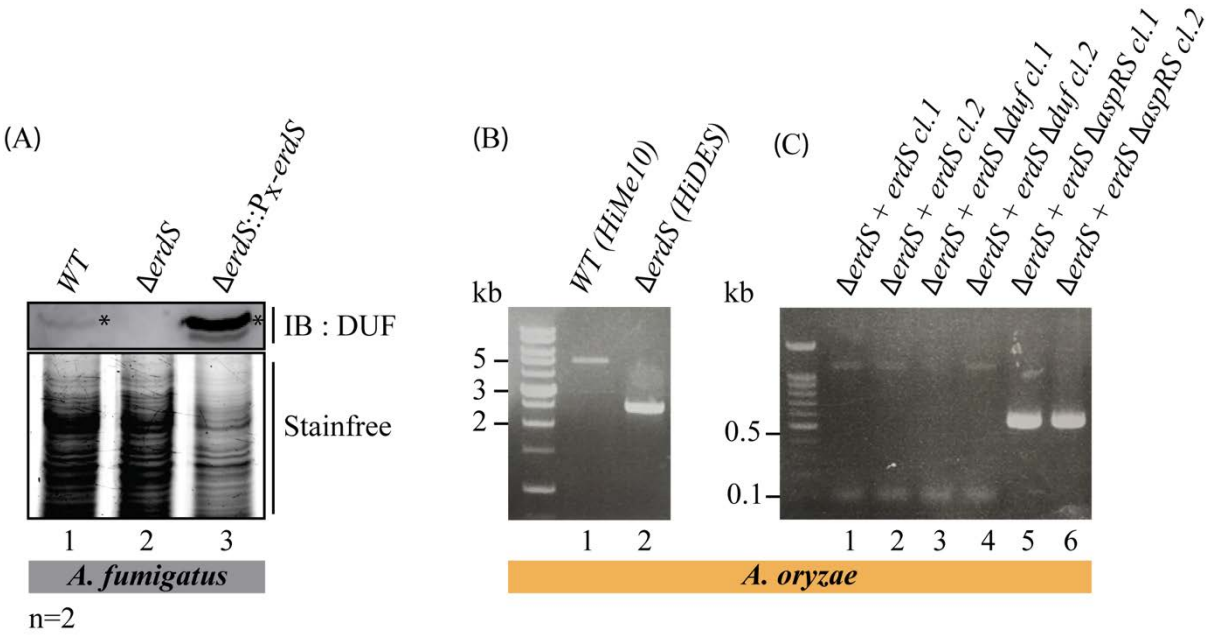

Figure S2: (**A**) Confirmation of *erdS* deletion in Δ*erdS* (lane 2) and complementation in Δ*erdS::*P*x-erdS* (lane 3) extracts using immunodetection of ErdS with anti-ErdS polyclonal antibodies (WT as a control) (n=2). Stainfree: loading control. The uncropped Western Blot is shown in **Figure S8**. (**B**) Confirmation of the presence of*erdS* in *Aor* HiMe10 (lane 1) and *erdS* deletion in *Aor*HiDES (lane 2) by PCR amplification. (**C**) PCR confirmation of Δ*erdS* complemented with *erdS* (lanes 1 and 2), *erdS*Δ*duf* (lanes 3 and 4) or *erdS*Δ*aspRS* (lanes 5 and 6) in *Aor* HiDES. Molecular weight markers are indicated in kb. Primers used for construction verification are listed in **Table S1 and S2**.

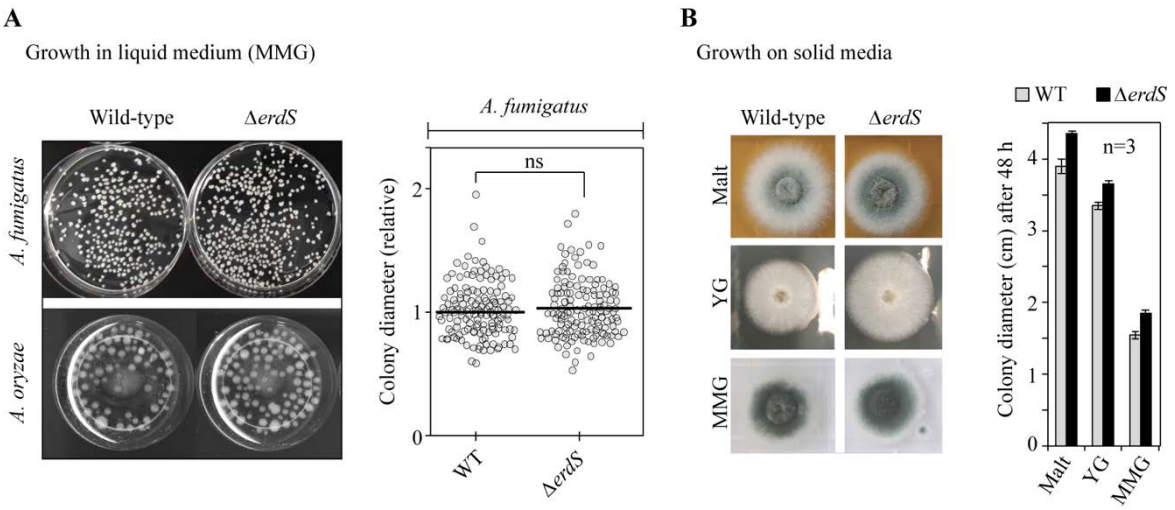

Figure S3: The *erdS* gene is not essential and its deletion does not affect growth or colony morphology. **(A)***A. fumigatus* and *A. oryzae* WT and Δ*erdS* strains were grown in liquid media under agitation (200 rpm) at 37°C and the resulting spherical colonies (pellets) obtained after 24 hrs were photographed (left panel). In the case of *Afm*, 140 colonies (pellets) of the WT and Δ*erdS* strains were measured (pixel area of individual pellets) and each represented in a dot plot. The geometric mean of pellets' sizes of the WT strain was normalized to 1. No significant (ns, t-test) differences were detected between both strains, indicating the absence of growth defects in the Δ*erdS* strain. **(B)** Growth was also analyzed on solid agar plates containing 3 different media: Malt extract, YG (Yeast extract 0.5 % (w/v), Glucose 2 %) and MMG (*Aspergillus* minimal medium with 1 % glucose). Six µL of a freshly prepared 10^6 conidia/mL suspension were spotted on plates and growth monitored (37 °C) up to 4 days. Results after 48 hours of growth are represented. Colony diameters of mycelia were monitored. No significant difference between the WT and Δ*erdS* strains was detected, indicating that mycelia expansion is not significantly altered upon deletion of the *erdS* gene in *Afm*.

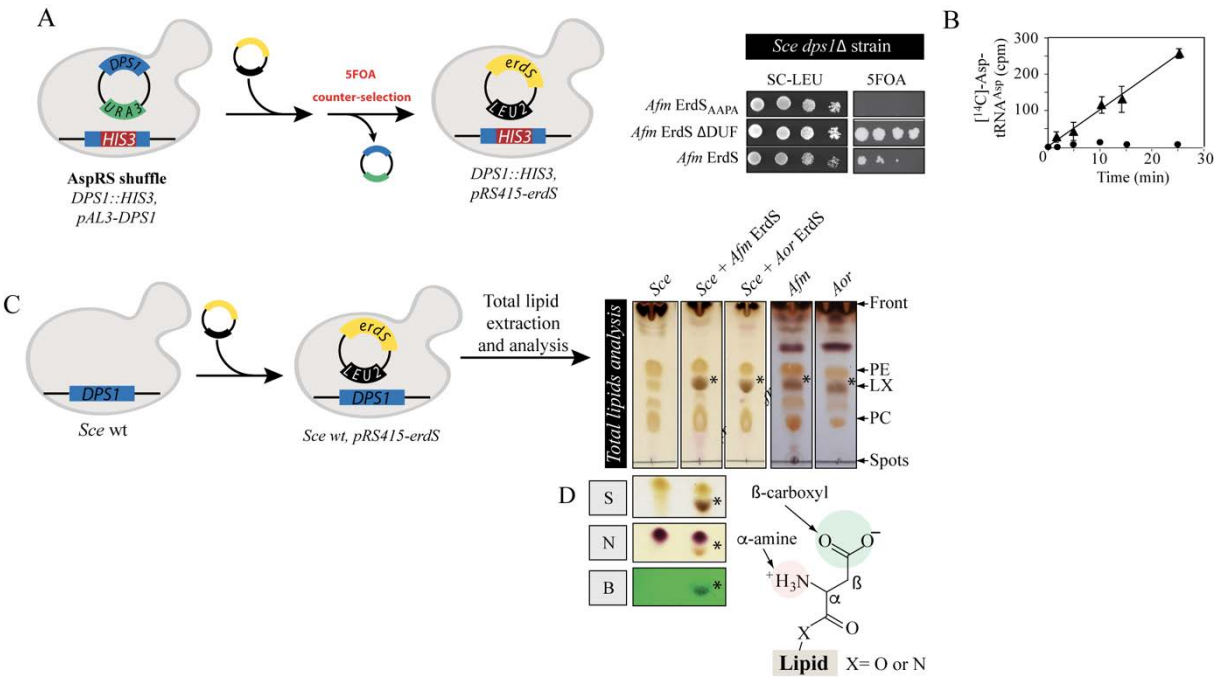

Figure S4:(**A**) Plasmid shuffling experiments in the Δ*dps1 Sce* strain. Drop tests were performed on SC-LEU and 5FOA media with Δdps1 strains carrying plasmids expressing the indicated *Afm* ErdS isoform: ErdS$_{AAPA}$ corresponds to ErdS mutated in the QSPQ motif of the AspRS domain, ErdS ΔDUF corresponds to ErdS with the DUF2156 domain deleted and ErdS corresponds to the full-length protein version. (**B**) *In vitro*tRNA^{Asp} aminoacylation assay performed with purified recombinant *Afm* ErdS (triangles) in the presence of pure *Sce* tRNA^{Asp}, ATP, and [^{14}C]-Asp. Circles: control without enzyme. (**C**) Total lipids were extracted from the 3 indicated *Sce* strains and from *Afm* and *Aor*, separated by TLC in the $CHCl_3$: MeOH: H_2O (130:50:8 v/v/v) solvent and stained with a $MnCl_2$/sulfuric acid treatment. The novel ErdS-dependent lipid (lipid X (LX), marked with *), also present naturally in *Afm* and *Aor* was detected. PE: phosphatidylethanolamine, PC: phosphatidylcholine. (**D**) An Asp residue is likely linked to any lipid via an ester (α-COO^-) or amide (N-containing) bond and have free α-NH_3^+ and β-COO^- groups. TLCs of total lipids extracted from *Sce* strain expressing *Afm* ErdS were stained with $MnCl_2$/sulfuric acid (S), ninhydrin (N) or bromocresol green (B) dyes and supported that lipid X contained an amine and carboxyl groups.

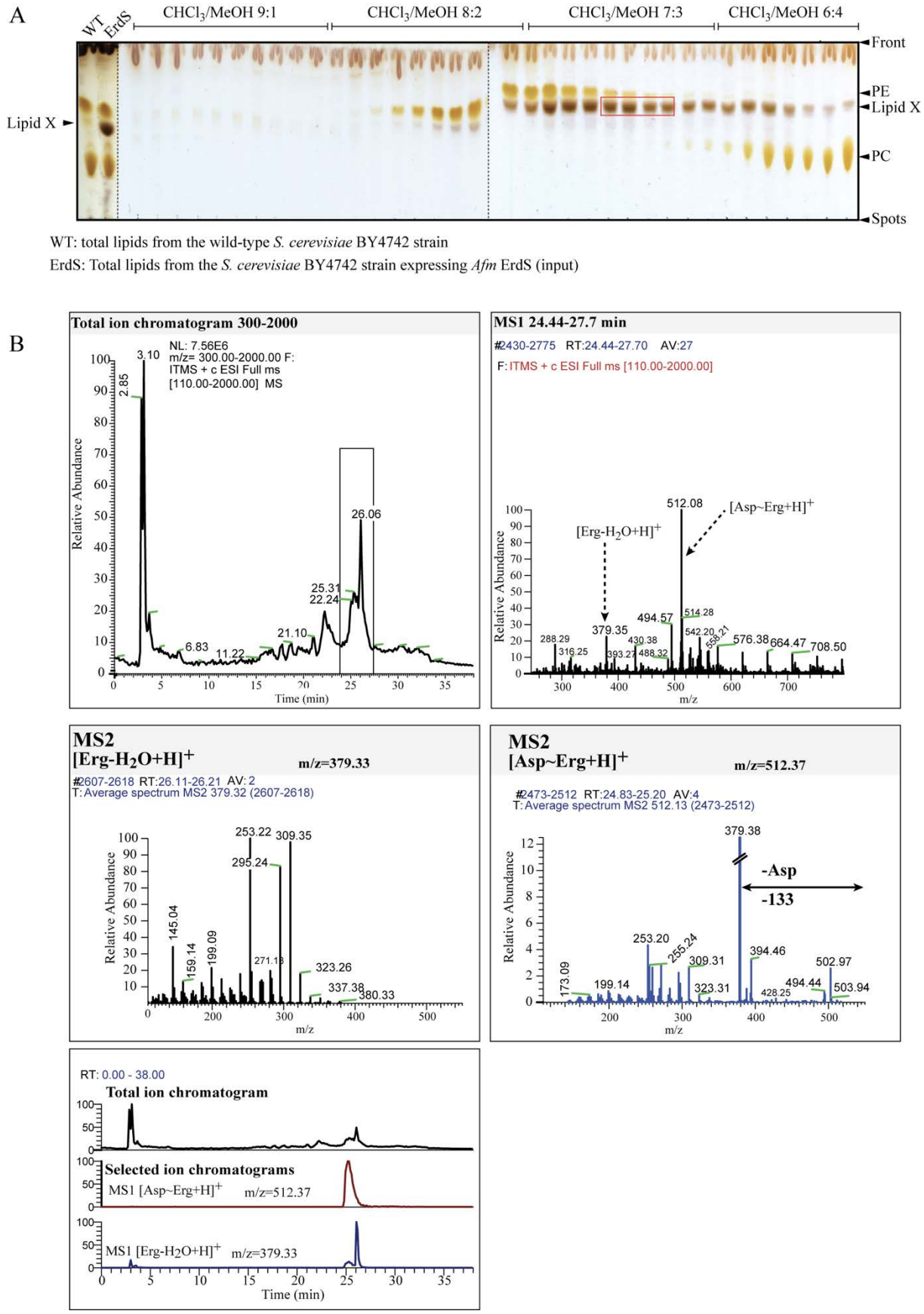

Figure S5: Purification of Erg-Asp from *Sce* and detection of Erg-Asp in total lipids from *Afm*. (**A**) Erg-Asp was purified from *Sce* expressing the *Afm* ErdS protein. Total lipids were loaded

on a silica gel 60 glass column, washed with $CHCl_3$, followed by acetone, and polar lipids were eluted using $CHCl_3$/MeOH mixture varying from 9/1 to 6/4 ratio. Fractions enriched in Erg-Asp were collected, pooled, and analyzed by MS/MS. Total lipids from a WT *Sce* strain that does not produce Erg-Asp were treated equally, and fractions corresponding to the elution peak of Erg-Asp were collected, pooled and used as a negative control for MS/MS (see **Fig. 4**). (**B**) In parallel, total lipids from *Afm* were extracted and directly analyzed. The figure shows the LC-ESI-MS/MS analysis of total lipid extract from *Afm*. 10 µL of total lipids from *Afm* were analyzed with a liquid chromatograph Surveyor Plus coupled with a LTQ-XL ion trap analyzer (Thermo Finnigan). The column was a Cogent Diamond Hydride (250×4.6 mm, 4 µm, Microsolv, Eatontown, NJ, USA) ran in hydrophilic interaction chromatography (HILIC) conditions. Mass spectrometer was run in positive mode, and MS/MS spectra were acquired for the 15 most intense peaks. Erg-Asp and Erg were identified with their MSMS spectra. Selected ion chromatograms show that these lipids had a retention time of 24.1 and 26.1 min, respectively.

A

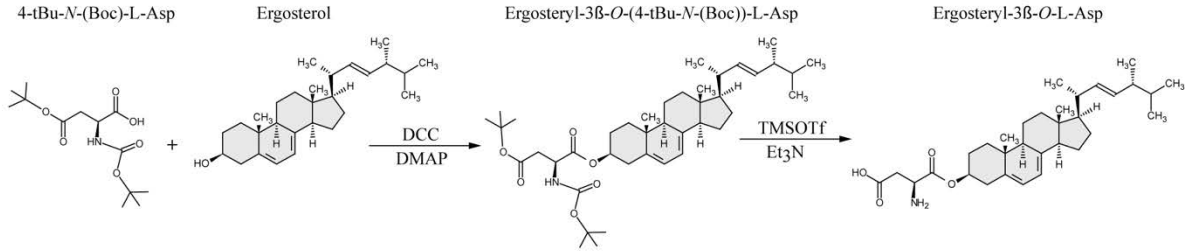

B

position	^{1}H(ppm)	^{13}C(ppm)	position	^{1}H(ppm)	^{13}C(ppm)
1		38,240	**17**		57,047
2		29,436	**18**	0.668, s	12,511
3		76,965	**19**	0.981, s	16,506
4		41,807	**20**		40,287
5		139,166	**21**	1.057, d	21,652
6	5.573, m	119,660	**22**	5.228, m	133,256
7	5.396, m	117,531	**23**	5.228, m	136,980
8		142,791	**24**		44,347
9		47,397	**25**		30,735
10		37,253	**26**	0.868, d	20,082
11		22,071	**27**	0.847, d	20,468
12		38,922	**28**	0.944, d	18,207
13		43,936	**1'**		172,663
14		55,691	**2'**	4.307, m	50,603
15		24,019	**3'**		34,368
16		28,844	**4'**		168,89

D

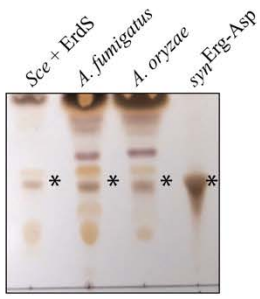

* Erg-Asp

Solvent system:
$CHCl_3$:MeOH:H_2O (130/50/8)

C

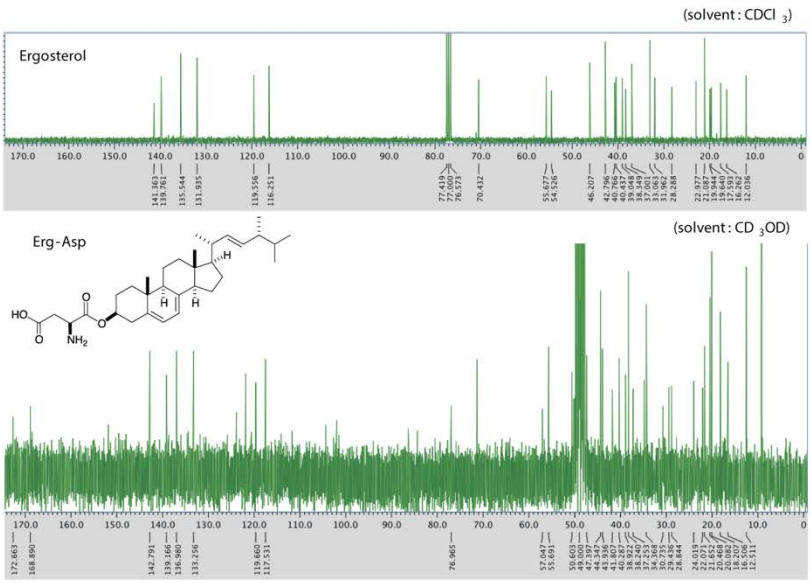

Figure S6: Chemical synthesis of Erg-Asp. (**A**) Two-step synthesis scheme of Erg-Asp (Ergosteryl-3β-*O*-L-aspartate) from Erg and 4-tBu-*N*-(Boc)-L-Asp. (**B**, **C**) NMR chemical shift assignments of synthetic Erg-Asp ($_{syn}$Erg-Asp) and [^{13}C] NMR spectrum of synthetic ergosteryl-3β-*O*-L-aspartate. (**D**) Comparison of $_{syn}$Erg-Asp (lane 4) with Erg-Asp extracted from a *Sce* strain expressing *Afm*ErdS (lane 1), from *Afm* and *Aor* (lanes 2, 3).

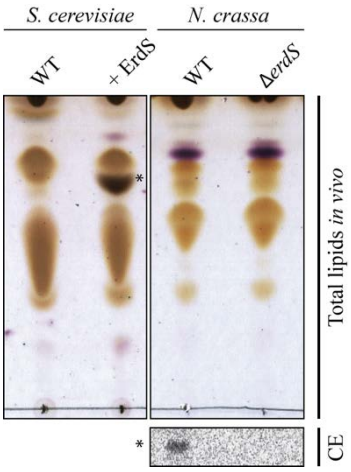

Figure S7: Total lipids from WT and Δ*erdS* strains of *Ncr* were extracted and separated by TLC with the $CHCl_3$(n=2): MeOH: H_2O (130:50:8 v/v/v) solvent and stained with a $MnCl_2$/sulfuric acid treatment. Control Sce strains that express (+) or not (WT)ErdS were used as controls. Erg-Asp is marked with *. The expression of ErdS was tested in crude protein extracts (CE) from the WT and Δ*erdS* strains of *Ncr* using the LA assay with [^{14}C]-Asp to monitor Erg-[^{14}C]Asp synthesis (n=2). To obtain a clear visualization of the Erg-[^{14}C]Asp band, after reaction and separation in TLC, at least 8 hrs of exposure (phosphorimaging) were required, which suggested that ErdS was weakly expressed or that a putative Erg-Asp hydrolase was expressed and masked ErdS activity by cleaving the Erg-[^{14}C]Asp product.

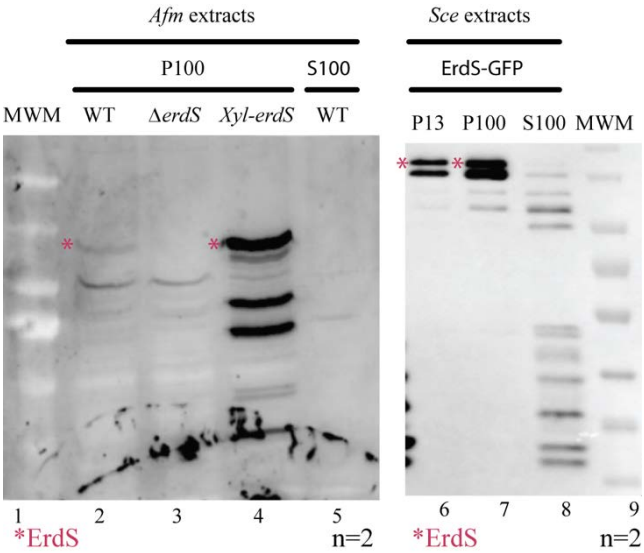

Figure S8: *Afm* ErdS colocalizes with membrane fractions. Western blot using anti-ErdS antibodies (1/1000 dilution) after 12 % SDS-PAGE (n=2). Lanes 1 &9: molecular weight marker; lanes 2 and 5: P100 andS100 fractions of the *Afm* WT strain extract; lane 3: P100 fraction of the *Afm* Δ*erdS* strain extract; lane 4: P100 fraction of an extract of the *Afm* Δ*erdS* strain complemented with the *erdS* gene under the dependence of a xylose promoter (overexpresses ErdS in the presence of xylose); lanes 6-8: P13, P100 andS100 fractions of an extract of the *Sce* strain overexpressing *Afm* ErdS. Note that lanes 2-4 represent the uncropped Western blot shown in Figure S2.

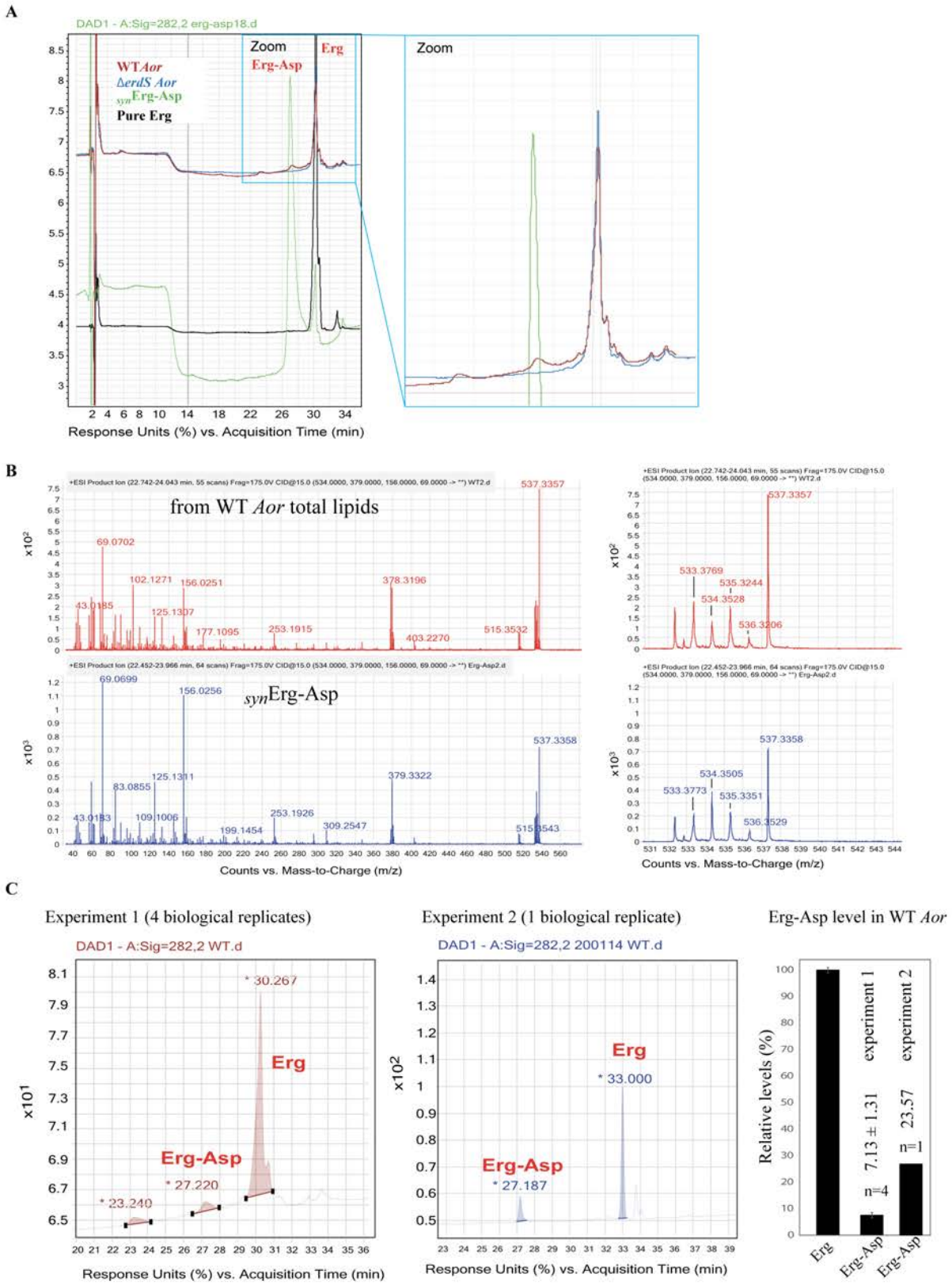

Figure S9:Detection and quantification of Erg-Asp in *Aor*.(A) Lipids extracted from *Aor* were fractionated on a TSKgel ODS80$_{TM}$ QA (C18) (2.0×150 mm, 5mm) column using a continuous gradient from 100 % MeOH:H_2O (4:1, v:v) (solvent A) to 100 % MeOH:CH_2Cl_2 (3:1, v:v)(solvent B) between 5 and 34 min at a flow rate of 0.2 mL/min at 25°C. Eluted compounds were monitored at 282 nm and

peaks of interest were submitted to an Accurate-Mass Q-TOF LC/MS (Agilent Technologies 6520) to confirm their identity **(B)** (upper spectrum: total lipids from WT *Aor* and bottom spectrum: $_{syn}$Erg-Asp). Lipids from a WT *Aor* strain (Erg and Erg-Asp present) and from a Δ*erdS* strain (no Erg-Asp) were analyzed and compared to the elution profile of pure Erg or of our synthetic (chemically synthesized) $_{syn}$Erg-Asp, as a reference (**A** and **B**).**(C)** Lipids from a WT *Aor* strain, having both Erg and Erg-Asp, were analyzed on a TSKgel ODS80$_{TM}$ QA (C18) (2.0×150 mm, 5mm) column with a continuous gradient from 100 % solvent A to 100 % B between 5 and 34 min and analyzed with an Accurate-Mass Q-TOF LC/MS (Agilent Technologies 6520) (experiment 1, 4 independent biological replicates). Quantification of peaks area showed that Erg-Asp represents 7.13±1.31 % of total Erg. Total lipids were also analyzed on a TSKgel ODS80$_{TM}$ QA (C18) (2.0×150 mm, 5mm) column in an independent biological replicate (experiment 2). In this case, quantification showed that Erg-Asp represented 27.2 % of total Erg. Discrepancies likely come from the solubility properties of Erg-Asp in extraction solvents, the amount found in experiment 2 representing an upper limit. Therefore, Erg-Asp is seemingly produced under standard growth conditions at levels between 7 and 20 %, but most likely ~10 % of total free Erg in *Aor*, which is in good correlation with TLC profiles obtained with *Aor* total lipids, but also with its close relative *Afm*.

Supplemental Tables

Table S1: Bacterial and fungi strains used in this study

REAGENT or RESOURCE	SOURCE	IDENTIFIER
Bacterial and Virus Strains		
Escherichia coli XL-1 Blue:endA1 gyrA96(nalR) thi-1 recA1 relA1 lac glnV44 F'[::Tn10 proAB+ lacIq Δ(lacZ)M15] hsdR17(r_K- m_K+)	Agilent (Stratagene)	Catalog#200249
Escherichia coli Rosetta-2: strain B F– *ompT gal dcmlonhsdSB(rB⁻mB⁻) λ(DE3 [lacI lacUV5-T7p07 ind1 sam7 nin5]) [malB⁺]K-12(λ^S))*, carrying the pRARE2 plasmid	Merck Millipore	71400-3
Escherichia coli DH5α: F^- endA1 glnV44 thi-1 recA1 relA1 gyrA96 deoRnupG purB20 φ80dlacZΔM15 Δ(lacZYA-argF)U169, hsdR17(r_K^- m_K^+), λ^-	Invitrogen	C404003
Organisms/Strains		
Saccharomyces cerevisiae strains		
Saccharomyces cerevisiae BY4742*: MATα his3Δ1 leu2Δ0 lys2Δ0 ura3Δ0*	Euroscarf	
Saccharomyces cerevisiae YAL3 *Δdps1: MATa ura3-52 lys2-801am trp1-63 his3-200 leu2-1 ade2-450 ade3-1483 dps1::HIS3*	Dr. Gilbert Eriani	Ador *et al*, 1999
Saccharomyces cerevisiae BY4742*: MATα his3Δ1 leu2Δ0 lys2Δ0 ura3Δ0* + pRS415-*erdSAfm*	This paper	N/A
Saccharomyces cerevisiae BY4742*: MATα his3Δ1 leu2Δ0 lys2Δ0 ura3Δ0* + pRS415-*erdSAor*	This paper	N/A
Saccharomyces cerevisiae BY4742*: MATα his3Δ1 leu2Δ0 lys2Δ0 ura3Δ0* + pRS415-*erdS ΔDUF2156Afm*	This paper	N/A
Saccharomyces cerevisiae BY4742*: MATα his3Δ1 leu2Δ0 lys2Δ0 ura3Δ0* + pRS415-*erdSΔaspRSAfm*	This paper	N/A
Saccharomyces cerevisiae BY4742*: MATα his3Δ1 leu2Δ0 lys2Δ0 ura3Δ0* + pRS415-*erdS$_{AAPA}$Afm*	This paper	N/A
Saccharomyces cerevisiae BY4742*: MATα his3Δ1 leu2Δ0 lys2Δ0 ura3Δ0* + pRS414-*erdS ΔDUF2156Afm* (AspRSonly)+ pRS415-*erdS ΔaspRSAfm* (DUF2156 only)	This paper	N/A
Saccharomyces cerevisiae YAL3 *Δdps1: MATa ura3-52 lys2-801am trp1-63 his3-200 leu2-1 ade2-450 ade3-1483 dps1::HIS3* + pRS415-*erdSAfm*	This paper	N/A

Saccharomyces cerevisiae YAL3 *Δdps1: MATa ura3-52 lys2-801am trp1-63 his3-200 leu2-1 ade2-450 ade3-1483 dps1::HIS3* + pRS415-*erdSAor*	This paper	N/A
Saccharomyces cerevisiae YAL3 *Δdps1: MATa ura3-52 lys2-801am trp1-63 his3-200 leu2-1 ade2-450 ade3-1483 dps1::HIS3* + pRS415-*erdS ΔDUF2156Afm*	This paper	N/A
Saccharomyces cerevisiae YAL3 *Δdps1: MATa ura3-52 lys2-801am trp1-63 his3-200 leu2-1 ade2-450 ade3-1483 dps1::HIS3* + pRS415-*erdSΔaspRSAfm*	This paper	N/A
Saccharomyces cerevisiae YAL3 *Δdps1: MATa ura3-52 lys2-801am trp1-63 his3-200 leu2-1 ade2-450 ade3-1483 dps1::HIS3* + pRS415-*erdS$_{AAPA}$Afm*	This paper	N/A
Saccharomyces cerevisiae YAL3 *Δdps1: MATa ura3-52 lys2-801am trp1-63 his3-200 leu2-1 ade2-450 ade3-1483 dps1::HIS3* + pRS415-*erdS* W785A *Afm*	This paper	N/A
Saccharomyces cerevisiae YAL3 *Δdps1: MATa ura3-52 lys2-801am trp1-63 his3-200 leu2-1 ade2-450 ade3-1483 dps1::HIS3* + pRS415-*erdS* W785A *Afm*	This paper	N/A
Saccharomyces cerevisiae YAL3 *Δdps1: MATa ura3-52 lys2-801am trp1-63 his3-200 leu2-1 ade2-450 ade3-1483 dps1::HIS3* + pRS415-*erdS* W785H *Afm*	This paper	N/A
Saccharomyces cerevisiae YAL3 Δ*dps1: MATa ura3-52 lys2-801am trp1-63 his3-200 leu2-1 ade2-450 ade3-1483 dps1::HIS3* + pRS415-*er**d**S* R789A *Afm*	This paper	N/A
*Aspergillus fumigatus*strains		
Aspergillus fumigatus CEA17^{KU80}*: pyrG akuB::pyrG (ΔakuB^{KU80})*	Prof. J.-P. Latgé. Pasteur Institute, Paris, France	Da Silva Ferreira ME et al., 2006
Aspergillus fumigatus CEA17^{KU80}*Δer**d**S (hph): pyrG akuB::pyrG (ΔakuB^{KU80}) **erd**S::hph*	This paper	N/A
Aspergillus fumigatus CEA17^{KU80}*Δ**erd**S: pyrG akuB::pyrG (ΔakuB^{KU80}) Δ**erd**S* (hph cassette excised)	This paper	N/A
Aspergillus fumigatus CEA17^{KU80}*Δ**erd**S::P$_{xyl}$-**erd**S: pyrG akuB::pyrG (ΔakuB^{KU80}) Δ**erd**S::[5'-utr- P$_{xyl}$-**erd**S-trpCterm-hph-3'-utr]*	This paper	N/A
Aspergillus oryzae strains		
Aspergillus oryzae RIB40*: wild-type*	H. Nakajima. Meiji University, Tokyo, Japan	Kuroki Y *et al.*, 2002

Aspergillus oryzae HiMe10: *ΔligD::AnpyrG-300bp ΔpyrG*	H. Nakajima Meiji University, Tokyo, Japan	Kuroki Y *et al.*, 2002
Aspergillus oryzae HiDES*Δ**erd**S:* *ΔligD::AnpyrG-300bp,* Δ***pyrG,*** *Δ**AorErd**S::AnpyrG-300bp*	This paper	N/A
Aspergillus oryzae HiDEC *Δ**erd**S+aspRS:* *ΔligD::AnpyrG-300bp, ΔpyrG, ΔAo-e**rd**S::AnpyrG-300bp, niaD::(AoaspRSniaDAnpyrG)*	This paper	N/A
Aspergillus oryzae HiDEC *Δ**erd**S+duf2156:* *ΔligD::AnpyrG-300bp, ΔpyrG, ΔAo-e**rd**S::AnpyrG-300bp, niaD::(Aoduf2156 niaDAnpyrG)*	This paper	N/A
Aspergillus oryzae HiDEC ***ΔerdS+erd**S:* ***ΔligD::AnpyrG-300bp, ΔpyrG, ΔAoErdS::AnpyrG-300bp, niaD::(Aoerd**SniaDAnpyrG)*	This paper	N/A
Neurospora crassa strains		
Neurospora crassa 74-OR23-1VA : wild-type*, matA*	FGSC	FGSC #2489
*Neurospora crassa Δ**erd**S:**erd**S::hph, matA*	FGSC	FGSC #20236
*Neurospora crassa ΔeraH:**erd**H::hph, matA*	FGSC	FGSC #20235
Other fungal strains		
*Aspergillus flavus*CA14: *ΔpyrG Δku80*	FGSC	FGSC #A1421
Beauveria bassiana NRRL 20698*:* wild-type	ATCC	ATCC 90517
Schizophyllum commune H4-8*:* wild-type	FGSC	FGSC #9210
*Aspergillus niger:*wild-type	University of Strasbourg	N/A
*Candida albicans:*wild-type	University of Strasbourg	N/A
Candida parapsilosis:wild-type	University of Strasbourg	N/A
*Geotrichum candidum:*wild-type	University of Strasbourg	N/A
*Penicillium expansum:*wild-type	University of Strasbourg	N/A
*Penicillium camemberti:*wild-type	University of Strasbourg	N/A
*Alternaria alternata:*wild-type	University of Strasbourg	N/A
*Cryptococcus neoformans:*wild-type	University of Strasbourg	N/A

Final plasmid	DNA template	Primers (5' --> 3')
Construction of donor plasmids containing erdS variants - Gateway BP reactions		
pDONR221-erdS-afm_Sce_opt	pUC57-erdS-afm_Sce_opt	GW_s : GGGGACAAGTTTGTACAAAAAAGCAGGCTTCATG

(GW BP reaction)		
		GW_as : GGGGACTTTGTACAAGAAAGCTGGGTC
pDONR221-erdS-Δduf2156 (GW BP reaction)	pUC57-erdS-afm_Sce_opt	FF001 : GGGGACAAGTTTGTACAAAAAAGCAGGCTTCATGTCAATCAAGAGAGCATTATCC
		FF003 : GGGGACCACTTTGTACAAGAAAGCTGGGTCTCAAGGTGGAAAAGATTTTGGATC
pDONR221-erdS-ΔaspRS (GW BP reaction)	pUC57-erdS-afm_Sce_opt	dufssDRS_s : GGGGACAAGTTTGTACAAAAAAGCAGGCTTCatgAGACACCCTGAAAGTTCTACAATAGAACC
		GW_as : GGGGACTTTGTACAAGAAAGCTGGGTC
pDONR221-erdS-aor (GW BP reaction)	A. oryzaegDNA	GGGGACAAGTTTGTACAAAAAAGCAGGCTTCatgtccatcaaacgggccc
		GGGGACCACTTTGTACAAGAAAGCTGGGTCttagtcttcgaaaaagtgaagg
pDONR221-erdS-afm_Sce_opt (GW BP reaction)	pUC57-erdS-afm_Sce_opt	GW_s : GGGGACAAGTTTGTACAAAAAAGCAGGCTTCATG
		GW_as : GGGGACTTTGTACAAGAAAGCTGGGTC
pDONR221-erdS-Δduf2156 (GW BP reaction)	pUC57-erdS-afm_Sce_opt	FF001 : GGGGACAAGTTTGTACAAAAAAGCAGGCTTCATGTCAATCAAGAGAGCATTATCC
		FF003 : GGGGACCACTTTGTACAAGAAAGCTGGGTCTCAAGGTGGAAAAGATTTTGGATC
pDONR221-erdS-ΔaspRS (GW BP reaction)	pUC57-erdS-afm_Sce_opt	dufssDRS_s : GGGGACAAGTTTGTACAAAAAAGCAGGCTTCatgAGACACCCTGAAAGTTCTACAATAGAACC
		GW_as : GGGGACTTTGTACAAGAAAGCTGGGTC
pDONR221-erdS-aor (GW BP reaction)	A. oryzaegDNA	GGGGACAAGTTTGTACAAAAAAGCAGGCTTCatgtccatcaaacgggccc
		GGGGACCACTTTGTACAAGAAAGCTGGGTCttagtcttcgaaaaagtgaagg
pDONR221-erdS-afm_Sce_opt (GW BP reaction)	pUC57-erdS-afm_Sce_opt	GW_s : GGGGACAAGTTTGTACAAAAAAGCAGGCTTCATG
		GW_as : GGGGACTTTGTACAAGAAAGCTGGGTC
Construction of *S. cerevisiae* expression plasmids - isoThermal assembly		
pRS415-GPD-erdS-aor	pDONR221-erdS-aor	#101 : gaactagtggatcccccatcacaagtttGTACAAAAAAGCAGGCTTC
		#102 : cttgatatcgaattcctgcagcccatcaCCACTTTGTACAAGAAAGCTGGGTC
	pRS415-GPD-X (LR recombined plasmid)	#104 : tgatgggctgcaggaattcgatatcaag
		#103 : aaacttgtgatgggggatccactagttc
pRS415-GPD-erdS-afm	pDONR221-erdS-afm	#101 : gaactagtggatcccccatcacaagtttGTACAAAAAAGCAGGCTTC
		#102 : cttgatatcgaattcctgcagcccatcaCCACTTTGTACAAGAAAGCTGGGTC
	pRS415-GPD-X	#104 : tgatgggctgcaggaattcgatatcaag
		#103 : aaacttgtgatgggggatccactagttc
pRS415-GPD-erdS-Δduf2156	pDONR221-erdS-Δduf2156	#101 : gaactagtggatcccccatcacaagtttGTACAAAAAAGCAGGCTTC
		#102 : cttgatatcgaattcctgcagcccatcaCCACTTTGTACAAGAAAGCTGGGTC
	pRS415-GPD-X	#104 : tgatgggctgcaggaattcgatatcaag
		#103 : aaacttgtgatgggggatccactagttc
pRS415-GPD-erdS-ΔaspRS	pDONR221-erdS-ΔaspRS	#101 : gaactagtggatcccccatcacaagtttGTACAAAAAAGCAGGCTTC
		#102 : cttgatatcgaattcctgcagcccatcaCCACTTTGTACAAGAAAGCTGGGTC
	pRS415-GPD-X	#104 : tgatgggctgcaggaattcgatatcaag
		#103 : aaacttgtgatgggggatccactagttc

pRS415-AspRS$_{AAPA}$-DUF2156	pRS415-GPD-erdS-afm	FF048 : TTTTAGCCGCTGCTCCTGCTTTGGCAAAGCAAATGGCCATC
		FF049 : CTTTGCCAAAGCAGGAGCAGCGGCTAAAAATGCATCTCTACCG
pRS415-GPD-erdS-aor	pDONR221-erdS-aor	#101 : gaactagtggatcccccatcacaagtttGTACAAAAAAGCAGGCTTC
Construction of *E. coli* overexpression plasmids - isoThermal assembly		
pMtevGWA-erdS-afm	pDONR221-erdS-afm	#142 : GGTACCGGATCTTACATCACAAGTTTGTACAAAAAAGCAGGCTTC
		#134 : GTGGTGGTGGTGCTCGAGGTACATCAACTTTGTACAAGAAAGCTGGGTC
	pMtevGWA-X	#114 : TGATGTACCTCGAGCACCACCACCAC
		#135 : AAACTTGTGATGTAAGATCCGGTACC
pMtevGWA-erdS-Δduf2156	pDONR221-erdS-Δduf2156	#142 : GGTACCGGATCTTACATCACAAGTTTGTACAAAAAAGCAGGCTTC
		#134 : GTGGTGGTGGTGCTCGAGGTACATCAACTTTGTACAAGAAAGCTGGGTC
	pMtevGWA-X	#114 : TGATGTACCTCGAGCACCACCACCAC
		#135 : AAACTTGTGATGTAAGATCCGGTACC
pMtevGWA-erdS-ΔaspRS	pDONR221-erdS-ΔaspRS	#142 : GGTACCGGATCTTACATCACAAGTTTGTACAAAAAAGCAGGCTTC
		#134 : GTGGTGGTGGTGCTCGAGGTACATCAACTTTGTACAAGAAAGCTGGGTC
	pMtevGWA-X	#114 : TGATGTACCTCGAGCACCACCACCAC
		#135 : AAACTTGTGATGTAAGATCCGGTACC
pMtevGWA-AspRS$_{AAPA}$-DUF2156	pMtevGWA-erdS-afm	FF048 : TTTTAGCCGCTGCTCCTGCTTTGGCAAAGCAAATGGCCATC
		FF049 : CTTTGCCAAAGCAGGAGCAGCGGCTAAAAATGCATCTCTACCG
pMtevGWA-erdH	*Afm*Genomic DNA	NY119 : AAGCAGGCTTCATGGCCTCTCATGCCCCTC
		NY120 : gAAAGCTGGGTCCTATCTGTCAAAAATCGC
	pMtevGWA-X	NY121 : GACAGATAGGACCCAGCTTTcttgtacaaagtgg
		NY122 : ATGAGAGGCCATGAAGCCTGCTTTTTTGTACaaac
pMtevGWA-erdH-S153A	pMtevGWA-erdH	NY145 : TGAGTGGTTTCGCTGCGGGCGGCAACCTCGCTG
		NY146 : TTGCCGCCCGCAGCGAAACCACTCAGAGCAATTC
pMtevGWA-erdH-D277A	pMtevGWA-erdH	NY147 : TCTGCGAATGGGCTATGCTGATGAACGAGGGC
		NY148 : TTCATCAGCATAGCCCATTCGCAGATGTACAG
Deletion and complementation cassettes for *Afm* strains - isoThermal assembly		
pJET1.2-erdS délétion cassette *Afm*	pSK529 (Hartmann et al., 2010)	FF166 : TATAGGTCAATAGAGTATACTTATTTG
		FF167 : TATTATGCTCAACTTAAATGACCTAC
	*Afm*CEA17ΔakuB^{KU80}gDNA	FF168 : cccgggTACGTTGGTACGTGAAAGAAATGG
		FF169 : TAAGTATACTCTATTGACCTATAGGTGACGGATGAGAGACCACC
		FF170 : GGTCATTTAAGTTGAGCATAATAAGTGGCAGATGTACCAAGCCC
		FF171 : cccgggTACGCCGCCTCCCTTCCCATTGC
pJET1.2-Pxyl-erdS	pJET1.2-erdS deletion cassette *Afm*	FF271 : CAAAGCACGTTTGATCGACATCTGCAgttggttcttcgagtcgatgaatg
		FF272 : TGCACTTCTTTGAAGACTAAGGATCCCCGACGCCGACCAACACCGCC
	Afm CEA17ΔakuB^{KU80}gDNA	FF273 : ATGTCGATCAAACGTGCTTTGTCTAAG
		FF274 : TTAGTCTTCAAAGAAGTGCAGAACCG
pJET1.2-erdS délétion cassette *Afm*	pSK529 (Hartmann et al., 2010)	FF166 : TATAGGTCAATAGAGTATACTTATTTG
		FF167 : TATTATGCTCAACTTAAATGACCTAC
	*Afm*CEA17ΔakuB^{KU80}gDNA	FF168 : cccgggTACGTTGGTACGTGAAAGAAATGG
		FF169 : TAAGTATACTCTATTGACCTATAGGTGACGGATGAGAGACCACC
		FF170 : GGTCATTTAAGTTGAGCATAATAAGTGGCAGATGTACCAAGCCC
***Afm* ΔerdS strains verification**		
	*Afm*CEA17ΔakuB^{KU80}gDNA	FF684 : GGAGATTGGATATGGATGAAGTGAAC
		FF685 : GTTGCCAACGTCGAGAAAACC
		NY15 : GAGCTGATGCTTTGGGCCGAGGACTGC
		NY16 : GCAGTCCTCGGCCCAAAGCATCAGCTC
	*Afm*CEA17ΔakuB^{KU80}gDNA	FF684 : GGAGATTGGATATGGATGAAGTGAAC
		FF685 : GTTGCCAACGTCGAGAAAACC
		NY15 : GAGCTGATGCTTTGGGCCGAGGACTGC

		NY16 : GCAGTCCTCGGCCCAAAGCATCAGCTC
Deletion and complementation cassettes for *Aor* strains - restriction and ligation		
pTAnpyrG	*A. nidulans* A26	AnpyrG-F : CCCCCCCGGGCTAGGCGCAATCCCTG
		AnpyrG-R : GGGGACTAGTGCCGGCTTAACCACAG
pAnpyrG-MR	pTAnpyrG	AnpyrG-SpeI-FF : CCCCACTAGTCTCGTCGGCTCTTTTCGCAA
		AnpyrG-SphI-FR : GGGGGCATGCGTAGAGGGTGCGGAGAACA
pUCdn	*Aor*RIB40*genomic DNA*	AoErdS-3′-SmaI-F : GACTAACCCGGGGCCTTCTTATGTTAGGCGTTTG
		AoErdS-3′-EcoRI-R : CTAGTCGAATTCTTCGAACCAGAATTAACGCTAC
pUCflk	*Aor*RIB40*genomic DNA*	AoErDS-5′-HindIII-F : ACCTGCAAGCTTCTTTAATATCCCGAGAATACTCG
		AoErDS-5′-PstI-R : TGATGACTGCAGTTGTGTAGCGGACGATAG
pDAor-ErDS	pAnpyrG-MR	AnpyrG-MR-SmaI-F primer : CTTCATCCCGGGCTAGGCGCAATCCCTGTC
		AnpyrG-MR-PstI-R primer : CTTCATCCCGGGCTAGGCGCAATCCCTGTC
pTAnpyrG	*A. nidulans* A26	AnpyrG-F : CCCCCCCGGGCTAGGCGCAATCCCTG
		AnpyrG-R : GGGGACTAGTGCCGGCTTAACCACAG
pAnpyrG-MR	pTAnpyrG	AnpyrG-SpeI-FF : CCCCACTAGTCTCGTCGGCTCTTTTCGCAA
		AnpyrG-SphI-FR : GGGGGCATGCGTAGAGGGTGCGGAGAACA
pUCdn	*Aor*RIB40*genomic DNA*	AoErdS-3′-SmaI-F : GACTAACCCGGGGCCTTCTTATGTTAGGCGTTTG
		AoErdS-3′-EcoRI-R : CTAGTCGAATTCTTCGAACCAGAATTAACGCTAC
pUCflk	*Aor*RIB40*genomic DNA*	AoErDS-5′-HindIII-F : ACCTGCAAGCTTCTTTAATATCCCGAGAATACTCG
		AoErDS-5′-PstI-R : TGATGACTGCAGTTGTGTAGCGGACGATAG
Deletant and complemented *Aor* strains verification		
	HiMe10, HiDES (gDNA)	P1 : AoErdS-5'-HindIII-F : ACCTGCAAGCTTCTTTAATATCCCGAGAATACTCG
		P4 : AoErdS-3'-EcoRI-R : CTAGTCGAATTCTTCGAACCAGAATTAACGCTAC
	HiDES + erdS, HiDES + erdSΔduf (gDNA)	P15 : AoErdS-486-F : TGCCAAGCTGGTTTTCCTTG
		P16 : AoErdS-575-R : ATGGCGATGGAATTCTTGCC
	HiDES + erdSΔaspRS (gDNA)	P10 :AoErdS-PmaCI-R : AGACACGTGTTAGTCTTCGAAAAAGTGAAGGACAG
		P17 : AoErdS-2274F : GGCGATCCTTTGTGCGATTC

Supplemental Materials and Methods

Media and growth conditions

For routine growth and maintenance of *Aspergillus fumigatus (Afm)* and *Aspergillus oryzae (Aor)*, fresh conidia were spread on Malt extract agar (ThermoScientific) plates or slants and incubated at 37 °C (*Afm*) or 30 °C (*Aor*). Mycelia were then incubated 7 days for *Afm* or 10 days for *Aor* until they produced enough conidia. *N. crassa* (*Ncr*) was grown in Vogel's agar medium. Nutrient-rich (NR) liquid or agar medium was composed of glucose 4 % (w/v), peptone 1 % (w/v) and yeast extract (YG) 1 % (w/v) (with 1.5 % w/v agar for plates or slants). Standard *Aspergillus* minimal medium Glucose (MMG) was composed as follow: For 1 L, it contained glucose (1 % w/v), ammonium tartrate dibasic(0.92 g, 5 mM, *i.e.*, 10 mM ammonium), salts (10 mL of a 50 X solution containing KCl 26 g/L, $MgSO_4$ $7H_2O$ 26 g/L, KH_2PO_4 76 g/L) and trace elements (0.5 mL of a 1000 X solution containing: $FeSO_4$ $7H_2O$ 1 g, Na_2EDTA 10 g, $ZnSO_4$ $7H_2O$ 4.4 g, H_3BO_3 2.2 g, $MnCl_2$ $4H_2O$ 1 g, $CoCl_2$ $6H_2O$ 0.32 g, $CuSO_4$ $5H_2O$ 0.32 g and Na_2MoO_4 0.8 g for 200 mL adjusted at pH 6.5). For MMX media, it contained 1 % (w/v) xylose as the carbon source. Solid media contained 1.5 % (w/v) agar. Agar plates or slants were incubated at 37°C (*Afm*) or 30 °C (*Aor*, *Ncr*) in the dark for indicated periods of time. Liquid cultures were incubated in glass flasks at 37 °C for *Afm* or 30 °C for *Aor*, *Ncr* and

all other filamentous fungi tested under shaking (220 rpm) for 24 (*Afm*) to 48 h (other fungi), until enough cells or mycelia were produced. *Sce*, *Candida* spp. and *C. neoformans* (*Cne*) were grown in NR medium for 24 h at 30 °C under agitation (220 rpm).

Spores/conidia preparation

Spores from 7 days for *Afm* or 10 days-old for *Aor* Malt agar slants were resuspended by addition of 5 mL sterile Tween 20-H_2O (0.05 % v/v) and vortexing, then the conidia were filtered with Cell Strainer filters (EASY strainer™ Greiner Bio-One), and the concentration was determined with a hemacytometer. Conidia were stored in Tween 20-H_2O (0.05 % v/v) at 4°C in the dark up to 1 week. For *Ncr*, conidia were harvested and treated similarly using 1 M sterile sorbitol.

Mycelia harvesting from liquid cultures

Liquid cultures to produce mycelia were inoculated with 10^6 to 10^7 conidia/mL in 50 mL liquid MMG for *Afm* or NR for *Aor*, incubated for 24 h at 37 °C (*Afm*) or 30° C (*Aor*) in the dark under agitation (220 rpm). Mycelia were then filtrated through two layers of gauze, rinsed twice with 50 mL sterile H_2O, and squeezed to eliminate excess water. Mycelia were directly used to extract total lipids.

Construction of cassettes for *A. fumigatus*

For the construction of Δ*erdS*mutants of *Afm*, 1000 bp of the 5'-upstream and of the downstream regions were amplified by PCR (using primer pairs FF#168 + FF#169 andFF#170 + FF#171, respectively) from *Afm*CEA17Δ*akuB*^{KU80}genomic DNA. Primers contained a 25 bp sequence at the 3' and 5' extremities, respectively, to obtain sequence tags corresponding to the 5' and 3' extremities of the *six*-P_{xyl}-β*rec-trpC-hygB-six* resistance cassette (1) flanked by *Sma*I restriction sites. The *six*-P_{xyl}-β*rec-trpC-hygB-six* resistance cassette was amplified by PCR (FF#166 and FF#167), and the 3 resulting fragments were fused using the Gibson method as described (2) to obtain the 5'-UTR-*six*-P_{xyl}-β*rec-trpC-hygB-six*-3'-UTR cassette flanked by the *Sma*I restriction sites. This cassette was ligated into a pJET1.2 plasmid using the CloneJET PCR Cloning Kit (ThermoScientific) following the manufacturer's instructions, to obtain the pJET1.2-Δ*erdS*deletion plasmid. The integrity of the deletion cassette was checked by PCR and sequencing. Thexylose-inducible *erdS* complementation cassette was constructed by replacing the β- *rec* gene in the 5'-UTR-*six*-P_{xyl}-β*rec-trpC-hygB-six*-3'-UTR cassette by the

wild-type *erdS* gene, so that it is under the control of the xylose promoter (P_{xyl}) (3) and the *trpC* terminator. The pJET1.2-Δ*erdS* plasmid was reverse-amplified with primers FF#271 and FF#272 to obtain the pJET1.2-Δ*erdS* open plasmid (pJET1.2-*eraS*-β*rec*$^{0,\ open}$) deprived of the β-*rec* gene. This PCR fragment was submitted to *Dpn*I digestion at 37 °C, 1 h, to remove the pJET1.2-Δ*erdS* matrix and purified using the Nucleospin Gel and PCR clean-Up Kit (Marcherey-Nagel). The *erdS* gene was amplified from *Afm*CEA17 24 ΔakuB^{KU80}enomic DNA using primers FF#273 and FF#274 with 20 pb 5'- and 3'-tags corresponding to the flanking regions of the β-rec gene. The pJET1.2-*eraS*-β*rec*$^{0,\ open}$ and *erdS* fragments were fused using the Gibson procedure (2) to obtain the pJET1.2-P_{xyl}-*erdS* (precisely, the pJET1.2 plasmid containing the 5'-UTR-*six*-P_{xyl}-*erdS*-*trpC*-*hygB*-*six*-3'-UTR cassette) integration plasmid. This cassette was designed to be integrated by homologous recombination at the Δ*erdS* locus. Because the β-*rec* gene was removed, once integrated at the Δ*erdS* locus, the 5'-UTR-*six*-P_{xyl}-*eraS*-*trpC*-*hygB*-*six*-3'-UTR cassette could not be excised.

Construction of mutants and complemented strains in *A. fumigatus*

Deletion of the *erdS* gene was obtained through homologous recombination with the deletion cassettes described above. Transformations of *Afm* were performed by electroporation of swollen conidia essentially as described (4) and we used 10 µg of linearized (*Sma*I-digested) deletion plasmid.

From the primary hygromycin-resistant colonies, conidia were isolated on individual Malt agar plates containing 150 µg/mL hygromycin B. After 3 days, conidia from single isolated colonies were scrapped and transferred on Malt agar slants containing 150 µg/mL hygromycin B and incubated 5 days at 37 °C. Genomic DNA was extracted (5)from mycelium cultures of Δ*erdS* mutants and the disruption of the *Afm*-*erdS* gene was confirmed by PCR (Primers FF#684 + NY#015 and NY#016 + FF#685) and by Western-blot. The hygromycin resistance cassette was then self-excised as described (1) on xylose-containing MM, and clones verified by PCR with primers FF#684 and FF#685.

To complement this Δ*erdS* strain, P_{xyl}-*erdS* cassette was inserted at the Δ*erdS* locus with the same protocol but the cassette could not be excised since, for this construct, the β-recombinase gene (1) was replaced by the *erdS* open reading frame.

Construction of cassettes for *A. oryzae*

For the disruption of *Aor-erdS* in *Aor*, *pyrG* marker recycling method was used (6). The first 300 bp of the coding sequence (starting from the ATG codon) of *Aspergillus nidulanspyrG* was amplified (AnpyrG-300 bp) and ligated to the 3' end of *pyrG* gene, immediately after the stop codon. This will bring the first 300 bp sequence directly attached to the 3' end of the *pyrG* gene in tandem repeats. The *pyrG* gene was amplified by PCR from *A. nidulans* A26 genomic DNA with the primers AnpyrG-F and AnpyrG-R. The PCR product was then ligated into pT7Blue using TA-cloning kit to yield pTAnpyrG. AnpyrG-300bp was amplified from pTAnpyrG with the primers AnpyrG-SpeI-FF and AnpyrG-SphI-FR. The resulting fragment was ligated into pTAnpyrG digested with *Spe*I and *Sph*I to yield the pAnpyrG-MR.

To construct the *Aor-erdS* gene disruption cassette, the upstream (1.0 kb) and the downstream (1.0 kb) flanking region of *Aor-erdS* ORF were amplified by PCR from *Aor*RIB40 genomic DNA using primer pairs AoErDS-5'-HindIII-F and AoErDS-5'-PstI-R for the upstream, and AoErDS-3'-SmaI-F and AoErDS-3'-EcoRI-R for the downstream regions. The downstream fragment was ligated into pUC118 vector digested with *Sma*I and *EcoR*I to yield the pUCdn, and then the upstream fragment was ligated into pUCdn digested with *Hind*III and *Pst*I to yield the pUCflk. The AnpyrG-MR was amplified from pAnpyrG-MR with the primers AnpyrG-MR-SmaI-F and AnpyrG-MR-PstI-R, and ligated into pUCflk digested with *Sma*I and *Pst*I to yield the pDAor-ErDS.

Construction of mutants and complemented strains in *A. oryzae*

The conidial suspension of *Aor*HiMe10was inoculated in 50 mL GPYU broth (2 % glucose, 1 % polypeptone, 0.5 % yeast extract, 0.1 % uridine, 0.1 % uracil) and incubated for 18 h at 30 ˚C and 160 rpm. Then mycelia were harvested by filtration with sterile Myracloth, washed with sterile distilled water and the cell walls digested with 1 % yatalase (Takara), 0.6 M $(NH_4)_2SO_4$, 50 mM maleate buffer (pH 5.5) at 30 ˚C for 3 h. Protoplast conversion was monitored by microscopic observation. After removing hyphal debris by filtration, the protoplast suspension was diluted 1:1 with Solution I (1.2 M sorbitol, 50 mM $CaCl_2$, 35 mM NaCl, 10 mM Tris-HCl, pH 7.5). Protoplasts were collected by centrifugation (2000 rpm, 8 min, 4 ˚C) and washed twice with Solution I. Finally, protoplasts were resuspended in Solution I at $2x10^7$ cells mL^{-1}. Of the protoplast suspension, 200 µL was mixed with 15 µg of linearized disruption cassette and incubated on ice for 30 min, then to the mixture was added 1.35 mL Solution II (60 % PEG4000, 50 mM $CaCl_2$, 10 mM Tris-HCl, pH 7.5). After 20 min incubation at room temperature (RT), the mixture was diluted with 5 mL Solution I and centrifuged (2000 rpm, 8 min, 4 ˚C). The precipitates were suspended in 250 µL Solution I and added in 5 mL Top agar (selective media

including 1.2 M sorbitol and 0.8 % agar) and then the transformation mix overlaid on selective agar media (3 % sucrose, 0.3 % $NaNO_2$, 0.1 % K_2HPO_4, 0.05 % $MgSO_4 \cdot 7H_2O$, 0.05 % KCl, 0.001 % $FeSO_4 \cdot 7H_2O$ and 1.2 M sorbitol). The plates were incubated at 30 ˚C for seven days. From the primary transformation plates, conidia were isolated from individual colonies using a flamed loop and transferred on individual Czapek-Dox agar plates to allow isolated sporulating colonies to form. After isolating three times to a single colony, conidia were inoculated into 5 mL GPY broth and incubated for 18 h at 30 ˚C and 160 rpm. Mycelia were harvested by filtration through Miracloth, washed with water, subjected to genomic DNA extraction with the DNeasy Plant Mini Kit (Qiagen) following the manufacturer's instructions. After isolation, the disruption of the *Aor-eraS* gene was confirmed by PCR with QuickTaq HS DyeMix (TOYOBO)using primers AoEraS-F2 and AnpyrG-F2 that were designed based on homologous region and the AnpyrG-MR, respectively. The AnpyrG-MR was self-excised on PDU agar media containing 5-FOA. The resulting disruption mutant was named HiDES.

To complement the *Aor* Δ*eraS* disruption mutant, the plasmid pUAES was constructed, which harbors the *Aor-eraS* gene, the promoter region of *Aor-eraS* and the terminator of *agdA*. The *Aor-eraS* gene was amplified by PCR using the primers PEraS-Sse8387I-F and AoEraS-PmaCI-R digested with *Sse8387*I and *PmaC*I, and then ligated into pUenoP digested with *Pst*I and *Sma*I. The resulting pUAES plasmid containing the *niaD* gene was introduced into HiDES to obtain HiDEC. Clones were isolated and identified as described above.

Induction of *erdS* expression with xylose

Liquid cultures were performed as described in the previous section, and mycelia harvested similarly. Then washed mycelia were resuspended in fresh minimal media containing 1 % glucose (w/v) or 1 % xylose (w/v) as the sole carbon source, to induce or not ErdS and Erg-Asp overproduction in the Δ*erdS*::P_{xyl}-*erdS* strain of *Afm*. Mycelia were then harvested as described and lipids extracted as specified below.

Construction of *Sce* and *E. coli* expression plasmids

The *Afm erdS* open reading frame (*AFUA_1g02570*) was synthesized (Genscript®) with codon optimization for expression in *Sce*, amplified by PCR (Primers GW_s and GW_as) and cloned in a pDONR221-*ccdB* vector (kanamycin resistance marker) (Gateway technology) using a BP reaction as described (7). To construct the *erdS*Δ*duf2156* and *erdS*Δ*aspRS* variants, the *erdS* sequence was amplified with primers pairs FF#001/FF#003 and

Dufssdrs_sens/GW_as, respectively, that contained *attB1* and *attB2*5'-tags, and introduced in the pDONR221-*ccdB* with a BP reaction, as described (7). To transfer the *erdS*, *erdS*Δ*duf2156* and *erdS*Δ*aspRS* constructs in destination vectors (pDEST was pRS415-Gpd or pRS414-Gpd), we first amplified the corresponding ORFs from the pDONR vectors with primers #101 and #102. We reverse-amplified a pDEST vector containing another unrelated ORF (already recombined) with primers #104 and #103 to obtain the open form of the plasmid without this unrelated ORF. Fragments (*erdS*, *erdS*Δ*duf2156* and *erdS*Δ*aspRS*) were introduced in the open pDEST form separately using the Gibson assembly procedure as described (2) and recombinant plasmids verified by PCR, restriction analysis and sequencing. The same procedure was used to clone the *erdS* gene from *Aor* (primers FF#099 and FF#100 to insert the ORF in the pDONR and primers #101 and #102 to transfer in the pDEST vectors).

To construct vectors enabling the expression of Maltose-binding protein fusions in *E. coli*, the codon-optimized *erdS* ORFs and variants were PCR-amplified using primers #142 and #134, and the pDEST (pMTevGWA) reverse-amplified with primers #114 and #135 before performing the Gibson assembly. The same was applied for the *erdH* gene (*AFUA_1g02580*, no introns) that was PCR-amplified from *Afm*KU80 with primers NY#119 and NY#120 and inserted directly in the pMTevGWA open vector generated by reverse-amplification with primers NY#121 and NY#122.

Site directed mutagenesis was performed with primer pairs containing selected mutations (indicated and described in supplementary table), as previously described (8).

Plasmid-shuffling complementation assays in *S. cerevisiae*

Plasmid shuffling experiments were conducted in the Δ*dps1 Sce* strain (9) rescued with a wild-type *DPS1* gene copy cloned in an *URA3*-bearing plasmid. All *Afm* or *Aor erdS* constructs to be tested were cloned in p415 (LEU) plasmids, transformed in the Δ*dps1* strain, and shuffled essentially as described (10, 11).

Proteins extraction and Western blots

For yeast crude extract preparation, 1 OD_{600nm} of cells were resuspended and incubated 10 min in 500 µL of pre-cooled NaOH 0.185 N, then precipitated by adding 50 µL of Trichloroacetic acid (TCA) 100 % and incubated 10 min on ice. Finally, the samples were centrifuged at 13, 000 x *g* for 15 min and the resulting pellets were resuspended in 100 µL of

Laemmli Sample Buffer. Then, 8 µL of each sample was then resolved on 10 % SDS-PAGE gels. Samples were separated by using a BioRad Mini-PROTEAN electrophoresis apparatus. For western blotting, proteins were transferred onto PVDF membranes that were blocked in 5 % (w/v) skimmed milk in TBS-Tween (TBS 1X, Tween-20 0.3 % (v/v)) for 1 h at RT. Primary antibodies (polyclonal anti-DUF2156, Covalab, France, anti-PGK) were incubated overnight at 4 °C and then washed several times with TBS-Tween. Membranes were then incubated for 1 h with HRP-conjugated secondary antibodies (Goat anti-rabbit for anti-DUF2156 and Goat anti-mouse for anti-PGK) at RT. Revelation was performed with the BioRad clarity western ECL Kit and monitored in a BioRad ChemiDoc Touch® apparatus.

Recombinant protein expression and purification

For recombinant protein purification, we modified the pMGWA vector (described in (7)) by introducing the Maltose Binding Protein (MBP) tag coding sequence 5' to a TEV cleavage site (TevCS). The gene encoding the protein of interest (*erdS*, *erdH* and mutants) was then cloned into this pMtevGWA using the above described cloning method. The resulting MBP-TevCS-X expression plasmids were then transformed in *E. coli* Rosetta-2 strains. Transformed bacteria were grown in LB medium containing ampicillin (150 µg/ml) and shaken at 37 °C, until an OD_{600nm} ~ 0.5-0.6 was reached. Cultures were then chilled on ice for 30 min and protein overexpression was induced with 0.1 mM IPTG for 12 h at 18 °C. Finally, cells were harvested by centrifugation (5000 x *g*, 15 min, 4 °C). The resulting cell pellet (~9 g) was resuspended in 30 mL of Tris-HCl pH 7 250 mM lysis buffer, containing NaCl 300 mM, KCl 30 mM, Glycerol 5 % (v/v), Tween 20 0.25 % (v/ v), TritonX-100 0.1 % (v/v), 2-mercaptoethanol 5 mM, Na_2EDTA 0.5 mM and a protease inhibitor cocktail (Roche Complete, EDTA-free). Cell lysis was performed by sonication (6 x 1 min, amplitude 28 %) (Vibracell, 72408) with intermediate cooling on ice. The lysate was centrifuged at 13, 000 x *g*, 20 min and the supernatant directly incubated with 1 mL of equilibrated amylose resin (NEB Amylose Resin, E8021S) at 4 °C on a rotating wheel. After transfer on an column (BioRad), the flow through was collected, beads where washed with 5 column volumes (CV) of wash buffer (Tris-HCl pH 7 50 mM, NaCl 300 mM, KCl 30 mM, Glycerol 5 % (v/v), Tween-20 0.25 % (v/v), 2-mercaptoethanol 10 mM) and the recombinant protein was eluted with 5 x 1 mL of elution buffer (Wash buffer supplemented with 2 % (p/v) of maltose monohydrate (Sigma-Aldrich). The collected fractions were then analyzed on 10 % SDS-PAGE gels. Fractions containing MBP-TevCS-X (X: ErdS, ErdH or mutants) protein were pooled. When required, the MBP-tag was cleaved off using the TEV

protease, as described. To separate the protein of interest from the MBP-tag and some other contaminants, fractions were injected on a HiLoad 16/600 Superdex 200 pg set up on a ÄKTA pure chromatography system (GE Healthcare). Finally, the fractions containing the protein of interest where pooled, concentrated to a final concentration of 1 mg/mL and stored at -20 °C with 30 % glycerol until use.

***S. cerevisiae* tRNA^{Asp} purification**

Extraction and purification of tRNA^{Asp} from *Sce* was performed as described elsewhere (12).

***In vitro*tRNA^{Asp}aspartylation assay**

Aspartylation of tRNA^{Asp} was performed as and adapted from (13, 14). Briefly, pure MBP-ErdS (or mutants) or ErdS (or mutants) without the N-terminal MBP tag were used. Aminoacylation reactions were performed in a Na-HEPES 100 mM pH 7.2 buffer containing KCl 30 mM, $MgCl_2$, 12 mM, ATP 10 mM, BSA 0.1 mg/mL, pure yeast tRNA^{Asp} (10 µM), [U-^{14}C]-Asp (280 cpm/pmol, Perkin Elmer) in a final volume of 100 µL. Reactions were initiated by adding 1 µg of enzyme pre-incubated at 30°C, and incubated at 30 °C. At each time points, 10 µL of reaction mix were removed, spotted onto Whatman paper filters (2 x 2 cm) and plunged into a 5 % TCA solution in a glass beaker to precipitate [^{14}C]-Asp-tRNA^{Asp}. Papers were washed 3 times for 15 min in 5 % TCA to remove residual free [^{14}C]-Asp, and 3 times 5 min in 100 % ethanol and air-dried. Radioactivity of precipitated [^{14}C]-Asp-tRNA^{Asp} was counted in a scintillation counter. Control experiments were performed with a reaction mix deprived of enzyme to obtain the background counts.

Chemical synthesis of ergosteryl-3β-*O*-L-aspartate and NMR analyses

4-*tert*-Butyl-1-ergosteryl *N*-(*tert*-butoxycarbonyl)-*L*-aspartate

Ergosterol (400 mg) and 4-*tert*-butyl-*N*-(*tert*-butoxycarbonyl)-*L*-aspartate (300 mg in Et_2O (30 ml)) at RT was added *N*,*N'*-dicyclohexylcarbodiimide (300 mg) and *N*,*N*-dimethyl-4-aminopyridine (amount of catalyst) and stirred for 3 h at RT. The mixture was extracted with EtOAc and washed with 1N HCl, sat. $NaHCO_3$ and sat. brine. The organic layer was dried over Na_2SO_4. Removal of the organic solvent *in vacuo* gave the crude product. Purification by silica gel column chromatography (hexane/EtOAc = 15:1) gave the product (480 mg) in 70 % yield. NMR was measured using JEOL ECP-500 (^{1}H at 500 MHz, ^{13}C at 125 MHz) with $CDCl_3$ (99.8% atom ^{2}H, Kanto Chemical, Japan) as a solvent with a solvent signal of δ 7.26 ppm for ^{1}H and δ 77.0 ppm for ^{13}C as references for chemical shifts.

^{1}H NMR (300 MHz, $CDCl_3$): δ 0.617 (s, 3H), 0.814 (d, *J* = 6.60 Hz, 3H), 0.830 (d, *J* = 6.60 Hz, 3H), 0.908 (d, *J* = 6.60 Hz, 3H), 0.940 (s, 3H), 1.028 (d, *J* = 6.60 Hz, 3H), 1.438 (s, 9H), 1.446 (s, 9H), 2.704 (dd, *J* = 4.40, 16.86 Hz, 1H), 2.887 (dd, *J* = 4.77, 16.86 Hz, 1H), 4.475 (m, 1H), 4.762 (m, 1H), 5.190 (m, 2H), 5.368 (m, 1H), 5.545 (m, 1H).

^{13}C NMR (75 MHz, $CDCl_3$): δ 12.022, 16.140, 17.571, 19.618, 19.930, 20.972, 21.073, 22.947, 28.020, 28.258, 28.291, 33.051, 36.405, 37.022, 37.786, 38.962, 40.417, 42.767, 42.768, 45.941, 50.192, 54.475, 55.642, 74.123, 79.861, 81.554, 116.214, 120.291, 131.941, 135.525, 138.197, 141.625, 155.518, 170.135, 170.653.

Ergosteryl-3β-*O*-L-aspartate

To 4-*tert*-Butyl-1-ergosteryl *N*-(*tert*-butoxycarbonyl)-*L*-aspartate (290 mg) in CH_2Cl_2 was added Et_3N (200 µL). After cooling with an ice bath, the mixture was added TMSOTf (300 µL) and stirred for 24 hrs at 0 °C. The mixture was extracted with $CHCl_3$ and washed with sat. $NaHCO_3$. The organic layer was dried over Na_2SO_4. Removal of the organic solvent *in vacuo* gave the crude product. Purification by silica gel column chromatography ($CHCl_3$ ~ $CHCl_3$/MeOH = 5:1) gave the product. NMR was measured with CD_3OD (99.8 % atom ^{2}H, Merck, Switzerland) as a solvent with a tetramethylsilane signal of δ 0.00 ppm for ^{1}H and a solvent signal of δ 49.0 ppm for ^{13}C as references for chemical shifts.

In silico analyses and determination of the phylogenomic distribution of ErdS

BLAST analyses

The protein sequence of the *Afm* AspRS-DUF2156 (ErdS) (encoded by the *AFUA_1G02570* gene in the Af293 strain) was used to perform PSI-BLAST searches (15) using non-redundant protein sequences databases and limited to fungi with 20,000 target sequences. Convergence was reached after 2 iterations. Sequences were then filtered using a home-made Python algorithm to recover only sequences of 250 to 2000 residues in length (7584 sequences) to exclude short and truncated versions of protein domains (AspRS and/or DUF2156). These filtered sequences were used to construct a protein size distribution plot in order to determine the average length of AspRS-DUF2156 proteins. Filtered sequences were then used to build a local BLAST database and a local BLAST search was performed using the sequence of the DUF2156 domain of *Afm* AspRS-DUF2156 as a query to detect DUF2156-containing proteins in the distribution plot (1006 sequences).

Phylogenomics analyses: To determine the phylogenomic distribution of AspRS-DUF2156 (ErdS), we used the *Afm* AspRS-DUF2156 sequence to retrieve by BLAST (15) all orthologs in each fungal class that belongs to the Dikarya sub-kingdom (Eurotio-, Lecanoro-, Xylono-, Dothideo-, Sordario-, Leotio-, Pezizo-, Orbioliomycetes, Saccharo- and Taphrinomycotina for ascomycetes, and in Agarico-, Puccinio- and Ustilagomycotina for basidiomycetes) and counted proteins containing a DUF2156 domain with length >750 residues, to take into account only complete and full-length AspRS-DUF2156 fusions, and not truncated forms that could account for sequencing or protein sequence prediction errors. No AspRS-DUF2156 fusions were detected outside Dikarya. We mapped the presence/absence of ErdS in each class onto the phylogenetic tree of fungi available at the JGI MycroCosm website (16). Distribution of ErdS was also monitored in the indicated selected species. In each case, we also indicated the presence of a canonical AspRS, involved in protein synthesis, for comparison.

Sequence alignments and analyses: Eleven ErdS (AspRS-DUF2156) protein sequences from *Aspergillus fumigatus*, *Aspergillus oryzae*, *Aspergillus flavus*, *Aspergillus niger*, *Penicilliumexpansum*, *Penicillium camemberti*, *Beauveria bassiana*, *Alternaria alternata*, *Neurosporacrassa*, *Cryptococcus neoformans* and *Schizophyllum commune* were used, together with 6 canonical AspRS sequences from *Saccharomyces cerevisiae*, *Candida albicans*, *A. fumigatus*, *A. oryzae*, *A. niger* and *N. crassa* to obtain a multiple alignment of all proteins with the Muscle program (17, 18) included in the Seaview package. Class II aaRS motifs 1, 2 and 3 (19) and the AspRS-specific QSPQ (20, 21) sequences were localized using the well characterized *S. cerevisiae*AspRS(20, 22). Residues known to be crucial for $tRNA^{Asp}$ acceptor arm, ATP, L-Asp or the Asp~AMP intermediate binding were identified according to the residues that had been experimentally identified in the yeast AspRS(9, 20, 23). The N-terminal extensions, AspRS and DUF2156 domains boundaries were determined according to the alignment.

Protein structure modelling and analysis: The amino acid sequence of the *Afm* AspRS-DUF2156 (ErdS) protein was used on the Phyre2 server (http://www.sbg.bio.ic.ac.uk/phyre2/html/page.cgi?id=index) (24) to obtain structurespredictions of either the AspRS (residues 1-593) or DUF2156 (residues 594-947) domains independently. Because sequence similarity with bacterial DUF2156 was very low (~20 %), the GNAT I and II subdomains – as well as the intercalated $\alpha^{(+)}$ helix – of the *Afm*DUF2156 (residues 594-947) were localized in the Phyre2 model by comparison with the

crystal structures of the DUF2156 domains of bacterial aaPGSs (25). The $\alpha^{(+)}$ helix of the DUF2156 domain was identified based on the model of the interaction inferred between $tRNA^{Ala}$ and the $\alpha^{(+)}$ helix of *P. aeruginosa* AlaPGS (25) where it was suggested to contact and recruit the Ala-$tRNA^{Ala}$ acceptor arm.

Supplemental References

1. T. Hartmann *et al.*, Validation of a self-excising marker in the human pathogen Aspergillus fumigatus by employing the beta-rec/six site-specific recombination system. *Appl Environ Microbiol***76**, 6313-6317 (2010).
2. D. G. Gibson *et al.*, Enzymatic assembly of DNA molecules up to several hundred kilobases. *Nat Methods***6**, 343-345 (2009).
3. I. Zadra, B. Abt, W. Parson, H. Haas, xylP promoter-based expression system and its use for antisense downregulation of the Penicillium chrysogenum nitrogen regulator NRE. *Appl Environ Microbiol***66**, 4810-4816 (2000).
4. K. Lambou, C. Lamarre, R. Beau, N. Dufour, J. P. Latge, Functional analysis of the superoxide dismutase family in Aspergillus fumigatus. *Mol Microbiol***75**, 910-923 (2010).
5. F. M. Muller *et al.*, Rapid extraction of genomic DNA from medically important yeasts and filamentous fungi by high-speed cell disruption. *J Clin Microbiol***36**, 1625-1629 (1998).
6. J. Maruyama, K. Kitamoto, Multiple gene disruptions by marker recycling with highly efficient gene-targeting background (DeltaligD) in Aspergillus oryzae. *Biotechnol Lett***30**, 1811-1817 (2008).
7. D. Busso, B. Delagoutte-Busso, D. Moras, Construction of a set Gateway-based destination vectors for high-throughput cloning and expression screening in Escherichia coli. *Anal Biochem***343**, 313-321 (2005).
8. S. N. Ho, H. D. Hunt, R. M. Horton, J. K. Pullen, L. R. Pease, Site-directed mutagenesis by overlap extension using the polymerase chain reaction. *Gene***77**, 51-59 (1989).
9. C. A. Ador L, Erbs P, Cavarelli J, Moras D, Gangloff J, Eriani G., Active site mapping of yeast aspartyl-tRNA synthetase by in vivo selection of enzyme mutations lethal for cell growth. *J Mol Biol***288**, 231-242 (1999).
10. L. Ador *et al.*, Active site mapping of yeast aspartyl-tRNA synthetase by in vivo selection of enzyme mutations lethal for cell growth. *J Mol Biol***288**, 231-242 (1999).
11. R. S. Sikorski, J. D. Boeke, In vitro mutagenesis and plasmid shuffling: from cloned gene to mutant yeast. *Methods Enzymol***194**, 302-318 (1991).
12. A. C. Dock *et al.*, Crystallization of transfer ribonucleic acids. *Biochimie***66**, 179-201 (1984).
13. F. Fischer *et al.*, The asparagine-transamidosome from Helicobacter pylori: a dual-kinetic mode in non-discriminating aspartyl-tRNA synthetase safeguards the genetic code. *Nucleic Acids Res***40**, 4965-4976 (2012).
14. H. Roy, M. Ibba, Monitoring Lys-tRNA(Lys) phosphatidylglycerol transferase activity. *Methods***44**, 164-169 (2008).
15. S. F. Altschul *et al.*, Gapped BLAST and PSI-BLAST: a new generation of protein database search programs. *Nucleic Acids Res***25**, 3389-3402 (1997).
16. I. V. Grigoriev *et al.*, MycoCosm portal: gearing up for 1000 fungal genomes. *Nucleic Acids Res***42**, D699-704 (2014).
17. R. C. Edgar, MUSCLE: a multiple sequence alignment method with reduced time and space complexity. *BMC Bioinformatics***5**, 113 (2004).

18. R. C. Edgar, MUSCLE: multiple sequence alignment with high accuracy and high throughput. *Nucleic Acids Res***32**, 1792-1797 (2004).
19. G. Eriani, M. Delarue, O. Poch, J. Gangloff, D. Moras, Partition of tRNA synthetases into two classes based on mutually exclusive sets of sequence motifs. *Nature***347**, 203-206 (1990).
20. E. G. Cavarelli J, Rees B, Ruff M, Boeglin M, Mitschler A, Martin F, Gangloff J, Thierry JC, Moras D (1994) The active site of yeast aspartyl-tRNA synthetase: structural and functional aspects of the aminoacylation reaction. in *EMBO J.*, pp 327-337.
21. B. H. Roy H, Reinbolt J, Kern D., When contemporary aminoacyl-tRNA synthetases invent their cognate amino acid metabolism. *Proc Natl Acad Sci U S A***100**, 9837-9842 (2003).
22. C. J. Eriani G, Martin F, Ador L, Rees B, Thierry JC, Gangloff J, Moras D., The class II aminoacyl-tRNA synthetases and their active site: evolutionary conservation of an ATP binding site. *J Mol Evol.***40**, 499-508 (1995).
23. K. S. Ruff M, Boeglin M, Poterszman A, Mitschler A, Podjarny A, Rees B, Thierry JC, Moras D., Class II aminoacyl transfer RNA synthetases: crystal structure of yeast aspartyl-tRNA synthetase complexed with tRNA(Asp). *Science***252**, 1682-1689 (1991).
24. L. Kelley, Mezulis, S, Yates, CM, Wass, MN, Sternberg, MJE (2015) The Phyre2 web portal for protein modeling, prediction and analysis. in *Nat Protocols*, pp 845-858.
25. S. Hebecker, Krauszeb,J , Hasenkampfa, T., Schneider, J., Groenewold, M., Reichelt, J., Jahn, D., Heinz, D.W., andMoser, J. (2015) Structures of two bacterial resistance factors mediating tRNA-dependent aminoacylation of phosphatidylglycerol with lysine or alanine. in *Proc Natl Acad Sci*, pp 10691–10696.